

Received May 11, 2022, accepted May 26, 2022, date of publication June 1, 2022, date of current version June 7, 2022.

Digital Object Identifier 10.1109/ACCESS.2022.3179573

# Dissipative Pinning Sampled-Data Control for Function Projective Synchronization of Neural Networks With Hybrid Couplings and Time-Varying Delays

THONGCHAI BOTMART<sup>1</sup>, WAJAREE WEERA<sup>1</sup>, ARTHIT HONGSRI<sup>1</sup>,  
NARONGSAK YOTHA<sup>2</sup>, AND PIYAPONG NIAMSUP<sup>3</sup>

<sup>1</sup>Department of Mathematics, Faculty of Science, Khon Kaen University, Khon Kaen 40002, Thailand

<sup>2</sup>Department of Applied Mathematics and Statistics, Rajamangala University of Technology Isan, Nakhon Ratchasima 30000, Thailand

<sup>3</sup>Department of Mathematics, Chiang Mai University, Chiang Mai 50200, Thailand

Corresponding author: Narongsak Yotha (narongsak.yo@rmuti.ac.th)

This work was supported by the Office of the Permanent Secretary, Ministry of Higher Education, Science, Research and Innovation, under Grant RGNS 63-113.

**ABSTRACT** This paper is concerned with the dissipative problem based pinning sampled-data control scheme. We investigate the problem for function projective synchronization of neural networks with hybrid couplings and time-varying delays. The main purpose is focused on designing a pinning sampled-data function projective synchronization controller such that the resulting function projective synchronization neural networks are stable and satisfy a strictly  $H_\infty, L_2 - L_\infty$ , passivity and dissipativity performance by setting parameters in the general performance index. It is assumed that the parameter uncertainties are norm-bounded. By construction of an appropriate Lyapunov-Krasovskii containing single, double and triple integrals, which fully utilize information of the neuron activation function and use refined Jensen's inequality for checking the passivity of the addressed neural networks are established in linear matrix inequalities (LMIs). This result is less conservative than the existing results in literature. It can be checked numerically using the effective LMI toolbox in MATLAB. Numerical examples are provided to demonstrate the effectiveness and the merits of the proposed methods.

**INDEX TERMS** Dissipative, function projective synchronization, neural networks, time-varying delays, sampled-data control.

## I. INTRODUCTION

For a long time, there has been a lot of interest in the study of artificial neural networks (NNs) because of their numerous applications, such as pattern recognition, image and signal processing, optimization, and so on [1]–[4]. Because time delay frequently occurs in many classes of NNs, it causes oscillation, degraded performance, divergence, and instability. Furthermore, time delay can be caused by the finite speed of information processing and the natural communication time between neurons. As a result, fruitful researchers have challenged the problem of delayed NNs [5]–[9].

The associate editor coordinating the review of this manuscript and approving it for publication was Shuai Liu<sup>1</sup>.

Furthermore, synchronization is one of many types of neural network behaviors that have a significant and appealing scenario. It has been studied in a variety of sciences [10]–[12]. To date, the literature has reported a wide range of synchronization phenomena, including complete synchronization (CS) [12], generalized synchronization (GS) [13], phase synchronization [14], anticipated synchronization [15], projective synchronization (PS) [16], and so on. Another type of function projective synchronization (FPS), has been introduced and studied [17], [18]. FPS is a broader definition of chaotic synchronization that encompasses both complete and projective synchronization. It states that the driver and response systems can be synchronized up to a scaling function [19], [20]. FPS has drawn the interest of

many researchers in plenty of fields [21]–[23]. FPS on memristive NNs has been proposed by Wu *et al.* in [21], where master-slave dynamical systems synchronize in case of weak and the desired scaling function. In [22], the drive-response systems can realize in FPS with linearly chaotic nodes, and a simple control law was applied. The exponential FPS of mixed delayed impulsive NNs was studied [23] using the contradiction method and analysis approach. In general, the systems cannot achieve synchronization autonomously due to weak coupling or variation in the NNs. As a result, we must artificially impose control from outside. Various control schemes can be applied in NNs such as adaptive control [24], [25], intermittent control [26], feedback control [27], impulsive control [28]. A natural method to achieve synchronization of networks is to input a controller to all network topology nodes. However, coupled NNs are typically composed of many-dimensional connected nodes, and controlling each node is difficult and expensive. To prevent part of nodes, named pinning control, was proposed in [29], many pinning rules have been applied in the synchronization of dynamical networks [30]–[32]. Due to, the skyrocketing in modern computers and communication, the controllers used to solve synchronization problems in continuous-time systems prefer to be digital. Thus, sampled-data control systems have received a lot of attention [33]–[36]. In such systems, digital computers are used to sample and calculate a continuous-time scale signal to generate a discrete-time signal, which is then converted back into a continuous-time control input signal utilizing a zero-order hold (ZOH) [37]. It is worth noting that the control signal is kept constant throughout the sampling period and is only allowed to change at the sampling instant. With the benefit of pinning and sampled-data control, so there are many of applications of pinning sample-data control. For example, [38] studied the problem of coupled reaction-diffusion neural networks with added inertia and time-varying delays. It can be synchronized by using pinning sampled-data approach. In [34], the problem of global  $H_\infty$  synchronization of complex networks based on pinning sampled-data control has been addressed. The  $H_\infty$  pinning synchronization of Lur'e complex networks with sampled-data control has been studied in [39]. However, few articles have been published on pinning function projective synchronization of connected NNs with hybrid couplings and time-varying delays at the same time. As a result, solving this problem for NNs is challenging.

Moreover, NNs have been investigated for a variety of analysis methods. In one research, the performance of NNs has been examined in a lot of approaches. The input and output relationships play a vital role in real-world problems. For example, Tang *et al.* [40] studied passive synchronization of coupled reaction-diffusion NNs with multiple time-varying delays by using an impulsive controller and Lyapunov theory. In [41], the research of passivity for NNs with an interval time-varying delay has been investigated by applying Lyapunov–Krasovskii function with double and triple integral terms and using new Jensen inequalities. And passivity

criteria for neural networks is published in [42]. Lu *et al.* [43]  $H_\infty$  synchronization of directed coupled NNs with mixed delays were examined using innovative criteria based on exceptional sampled-data control and the Lyapunov method. In [44], the problem of Takagi–Sugeno fuzzy NNs with  $L_2 - L_\infty$  filtering was addressed via Wirtinger-type inequalities, formulated in the restriction of LMI. As is known, the ingenious concept of dissipative analysis was first introduced by Willems [45]. It is noted that the dissipative performance has gotten more attention from researchers because it not only dealt with  $H_\infty$  and passivity performance [46], but it also indicates an excellent practicable control scheme in many varieties of sciences, including power converters [47] and chemical process control [48]. Recently, [49]–[52] has examined into  $(Q, S, R)$ -dissipativity analysis; however, in those works, the  $L_2 - L_\infty$  performance is not considered in the  $(Q, S, R)$ -dissipativity analysis. To address this concern, Zhang *et al.* [53] first introduced a general performance approach known as extended dissipativity, which involves these performances by adjusting weighting matrices in a unified framework. Furthermore, the study of extended dissipativity performance for NNs with time delays has been obtained more attention in the references [54]–[56]. As a result of incorporating the extended dissipative performance into the issue of synchronization for delayed coupled NNs, the analysis of the system will become more general, which has not yet been investigated.

By the above motivation, function projective synchronization and extended dissipativity performance are proposed for NNs with hybrid couplings and time-varying delays in this article. The main ideas of this work are given as follows:

- For the first time, we address the FPS problem for NNs including both discrete and distributed delays in the hybrid asymmetric coupling, which differs from the time-delay case in [57], [58]. Furthermore, the above delays are not necessarily differentiable functions, which can be easily be used into a real-world application. The output terms include the state vector with the disturbance and interval discrete time-varying delay.
- We develop a suitable Lyapunov–Krasovskii functional (LKF) for using in FPS stability and extended dissipativity analysis of delayed coupled NNs with new inequalities.
- We first obtained new FPS stability and extended dissipativity criteria that contain  $H_\infty$ ,  $L_2 - L_\infty$ , passivity, and dissipativity performance. New parameters in the general formulation has not yet been reported for delayed coupled NNs.
- Unlike previous work [59]–[61], we carefully study the FPS using mixed nonlinear and pinning sample-data controls for our control method.

The rest of paper is organized as follows: Section 2 provides some mathematical preliminaries and network model. Section 3 presents the passivity analysis of uncertain NNs with interval and distributed time-varying delays.

Numerical examples are given in Section 4. Finally, the conclusion is provided in Section 5.

**II. PROBLEM FORMULATION AND PRELIMINARIES**

*Notations:* Throughout this paper,  $\mathcal{R}^n$  denotes  $n$ -dimensional Euclidean space and  $\mathcal{R}^{n \times n}$  is the set of all  $n \times n$  real matrices. For any matrix  $X$ , the notation  $X > 0$  means that the matrix  $X$  is symmetric positive definite.  $\lambda_{\max}(X)$  and  $\lambda_{\min}(X)$  denote the maximum and minimum eigenvalues of  $X$ ,  $\text{sym}\{X\}$  means  $X + X^T$ . The superscript  $T$  stands for the transpose. The symbol  $*$  is used to represent the term of a symmetric matrix which can be inferred by symmetry. The symbol  $\otimes$  stands for Kronecker product and  $\text{diag}\{\dots\}$  denotes the block diagonal matrix.  $\mathcal{C}[-\varrho, 0], \mathcal{R}^n$  represents the space of all continuous vector functions mapping  $[-\varrho, 0]$  into  $\mathcal{R}^n$ , where  $\varrho \in \mathcal{R}^+$ .  $\mathcal{L}_2[0, \infty)$  denotes the space of functions  $\phi : \mathcal{R}^+ \rightarrow \mathcal{R}^n$  with the norm  $\|\phi\|_{\mathcal{L}_2} = [\int_0^\infty |\phi(\theta)|^2 d\theta]^{\frac{1}{2}}$ .

Given delayed NNs containing  $N$  identical nodes with hybrid couplings as follows:

$$\begin{aligned} \dot{y}_i(t) &= -Cy_i(t) + A_1f(y_i(t)) + A_2f(y_i(t - r(t))) \\ &\quad + A_3 \int_{t-d(t)}^t f(y_i(s))ds + \sigma_1 \sum_{j=1}^N g_{ij}^{(1)} B_1 y_j(t) \\ &\quad + \sigma_2 \sum_{j=1}^N g_{ij}^{(2)} B_2 y_j(t - r(t)) \\ &\quad + \sigma_3 \sum_{j=1}^N g_{ij}^{(3)} B_3 \int_{t-d(t)}^t y_j(s)ds + E_1 \omega_i(t) \\ &\quad + u_i(t), \\ \bar{z}_i(t) &= D_1 y_i(t) + D_2 y_i(t - r(t)) + E_2 \omega_i(t), \end{aligned} \tag{1}$$

$i = 1, 2, \dots, N$ , where  $y_i(t)$  and  $u_i(t)$  are the state variable and the control input of the node  $i$ , respectively.  $f(y_i(\cdot)) = (f_1(y_{i1}(\cdot)), f_2(y_{i2}(\cdot)), \dots, f_n(y_{in}(\cdot)))^T$  is a nonlinear vector valued function describing the dynamics of nodes.  $\bar{z}_i(t) \in \mathcal{R}^l$  is the measured output of the  $i$ th node,  $C = \text{diag}\{c_1, c_2, \dots, c_n\} > 0$  denotes the rate with which the cell  $i$  resets its potential to the resting state when being isolated from other cells and inputs.  $A_1, A_2$  and  $A_3$  are connection weight matrices,  $D_1, D_2, E_1$  and  $E_2$  are given real matrices, the positive constants  $\sigma_1, \sigma_2$  and  $\sigma_3$  are the strengths for the constant coupling and delayed couplings, respectively,  $\omega_i(t)$  is the system external disturbance which belongs to  $\mathcal{L}[0, \infty)$ ,  $B_1, B_2, B_3 \in \mathcal{R}^{n \times n}$  are inner-coupling matrices with constant elements and  $B_1, B_2, B_3$  are assumed as positive definite matrices,  $G^{(k)} = (g_{ij}^{(k)})_{N \times N} (k = 1, 2, 3)$  are the outer-coupling matrices and satisfy the following conditions  $g_{ij}^{(k)} \geq 0, i \neq j, g_{ii}^{(k)} = - \sum_{j=1, j \neq i}^N g_{ij}^{(k)}, i, j = 1, 2, \dots, N, k = 1, 2, 3$ . The interval discrete delay  $r(t)$  and distributed delay  $d(t)$  are satisfactory to the following conditions

$$0 \leq r_1 \leq r(t) \leq r_2, \quad 0 \leq d(t) \leq d, \tag{2}$$

where  $r_1, r_2$  and  $d$  are real constants. The isolated node of network (1) is given by the following delayed neural network:

$$\begin{aligned} \dot{w}(t) &= -Cw(t) + A_1f(w(t)) + A_2f(w(t - r(t))) \\ &\quad + A_3 \int_{t-d(t)}^t f(w(s))ds, \\ z_w(t) &= D_1w(t) + D_2w(t - r(t)), \end{aligned} \tag{3}$$

where  $w(t) = (w_1(t), w_2(t), \dots, w_n(t))^T \in \mathcal{R}^n$  and the parameters  $C, A_1, A_2, A_3, D_1, D_2$  and the nonlinear functions  $f(\cdot)$  have the same definitions as in (1). The network (1) is said to achieve FPS if there exists a continuously differentiable positive function  $\alpha(t) > 0$  such that

$$\lim_{t \rightarrow \infty} \|p_i(t)\| = \lim_{t \rightarrow \infty} \|y_i(t) - \alpha(t)w(t)\|, \tag{4}$$

$i = 1, 2, \dots, N$ , where  $\|\cdot\|$  stands for the Euclidean vector norm and  $w(t) \in \mathcal{R}^n$  can be an equilibrium point. Let  $p_i(t) = y_i(t) - \alpha(t)w(t)$ , be the synchronization error. Then, by substituting it into network (1), it is easy to get the following:

$$\begin{aligned} \dot{p}_i(t) &= \dot{y}_i(t) - \dot{\alpha}(t)w(t) - \alpha(t)\dot{w}(t), \\ &= -Cp_i(t) + A_1[f(y_i(t)) - \alpha(t)f(w(t))] \\ &\quad + A_2[f(y_i(t - r(t))) - \alpha(t)f(w(t - r(t)))] \\ &\quad + A_3 \int_{t-d(t)}^t [f(y_i(s)) - \alpha(t)f(w(s))] ds \\ &\quad + \sigma_1 \sum_{j=1}^N g_{ij}^{(1)} B_1 p_j(t) + \sigma_2 \sum_{j=1}^N g_{ij}^{(2)} B_2 p_j(t - r(t)) \\ &\quad + \sigma_3 \sum_{j=1}^N g_{ij}^{(3)} B_3 \int_{t-d(t)}^t p_j(s)ds - \dot{\alpha}(t)w(t) \\ &\quad + E_1 \omega_i(t) + u_i(t), \\ \hat{z}_i(t) &= D_1 p_i(t) + D_2 p_i(t - r(t)) + E_2 \omega_i(t), \end{aligned} \tag{5}$$

where  $\hat{z}_i(t) = \bar{z}_i(t) - z_w(t)$ .

Regarding to the pinning sampled-data control scheme, without loss of generality, the first  $l$  nodes are chosen and pinned with sampled-data control  $u_i(t)$ , expressed as the following form

$$u_i(t) = u_{i1}(t) + u_{i2}(t), \quad i = 1, 2, \dots, N, \tag{6}$$

where

$$\begin{aligned} u_{i1}(t) &= \dot{\alpha}(t)w(t) \\ &\quad - A_1[f(\alpha(t)w(t)) - \alpha(t)f(w(t))] \\ &\quad - A_2[f(\alpha(t)w(t - r(t))) \\ &\quad - \alpha(t)f(w(t - r(t)))] \\ &\quad - A_3 \int_{t-d(t)}^t [f(\alpha(t)w(s)) - \alpha(t)f(w(s))] ds, \\ &\quad i = 1, 2, \dots, N, \\ u_{i2}(t) &= \begin{cases} K_i p_i(t_k), & t_k \leq t < t_{k+1}, i = 1, 2, \dots, l, \\ 0, & i = l + 1, l + 2, \dots, N, \end{cases} \end{aligned} \tag{7}$$

where  $K_i$  is a set of the sampled-data feedback controller gain matrices to be designed, for every  $i = 1, 2, \dots, N$ ,  $p_i(t_k)$  is discrete measurement of  $p_i(t)$  at the sampling interval  $t_k$ . Denote the updating instant time of the zero-order-hold (ZOH) by  $t_k$  satisfy

$$0 = t_0 < t_1 < \dots < t_k < \lim_{k \rightarrow +\infty} t_k = +\infty, \\ t_{k+1} - t_k = \tau_k \leq \tau, \quad \forall k \geq 0, \quad (9)$$

where  $\tau > 0$  represents the largest sampling interval.

By substituting (6) into (5), it can be derived that

$$\begin{aligned} \dot{p}_i(t) = & -Cp_i(t) + A_1[f(y_i(t)) - f(\alpha(t)w(t))] \\ & + A_2[f(y_i(t-r(t))) - f(\alpha(t)w(t-r(t)))] \\ & + A_3 \int_{t-d(t)}^t [f(y_i(s)) - f(\alpha(t)w(s))] ds \\ & + \sigma_1 \sum_{j=1}^N g_{ij}^{(1)} B_1 p_j(t) \\ & + \sigma_2 \sum_{j=1}^N g_{ij}^{(2)} B_2 p_j(t-r(t)) \\ & + \sigma_3 \sum_{j=1}^N g_{ij}^{(3)} B_3 \int_{t-d(t)}^t p_j(s) ds + E_1 \omega_i(t) \\ & + K_i p_i(t-\tau(t)), \\ & i = 1, 2, \dots, l, \\ \dot{p}_i(t) = & -Cp_i(t) + A_1[f(y_i(t)) - f(\alpha(t)w(t))] \\ & + A_2[f(y_i(t-r(t))) - f(\alpha(t)w(t-r(t)))] \\ & + A_3 \int_{t-d(t)}^t [f(y_i(s)) - f(\alpha(t)w(s))] ds \\ & + \sigma_1 \sum_{j=1}^N g_{ij}^{(1)} B_1 p_j(t) \\ & + \sigma_2 \sum_{j=1}^N g_{ij}^{(2)} B_2 p_j(t-r(t)) \\ & + \sigma_3 \sum_{j=1}^N g_{ij}^{(3)} B_3 \int_{t-d(t)}^t p_j(s) ds + E_1 \omega_i(t), \\ & i = l+1, l+2, \dots, N, \end{aligned} \quad (10)$$

where  $\tau(t) = t - t_k$  satisfies  $0 \leq \tau(t) \leq \tau$ . The initial condition of (10) is defined by

$$p_i(\theta) = \phi_i(\theta), \quad -\varpi \leq \theta \leq 0, \quad (11)$$

where  $\varpi = \max\{r_2, d, \tau\}$  and  $\phi_i(\theta) \in \mathcal{C}[-\varpi, 0], \mathcal{R}^n$ ,  $i = 1, 2, \dots, N$ .

Let us define

$$K = \text{diag}\{\underbrace{K_1, K_2, \dots, K_l}_{l \text{ times}}, \underbrace{0_n, \dots, 0_n}_{N-l \text{ times}}\},$$

$$p(t) = \begin{bmatrix} p_1(t) \\ p_2(t) \\ \vdots \\ p_N(t) \end{bmatrix}, \quad \xi(p(\cdot)) = \begin{bmatrix} f(y_1(\cdot)) - f(\alpha(t)w(\cdot)) \\ f(y_2(\cdot)) - f(\alpha(t)w(\cdot)) \\ \vdots \\ f(y_N(\cdot)) - f(\alpha(t)w(\cdot)) \end{bmatrix}, \\ \omega(t) = \begin{bmatrix} \omega_1(t) \\ \omega_2(t) \\ \vdots \\ \omega_N(t) \end{bmatrix}, \quad z(t) = \begin{bmatrix} \hat{z}_1(t) \\ \hat{z}_2(t) \\ \vdots \\ \hat{z}_N(t) \end{bmatrix}.$$

Then, with Kronecker product, we can reformulate the system (10) as follows

$$\begin{aligned} \dot{p}(t) = & -(I_N \otimes C)p(t) + (I_N \otimes A_1)\xi(p(t)) \\ & + (I_N \otimes A_2)\xi(p(t-r(t))) \\ & + (I_N \otimes A_3) \int_{t-d(t)}^t \xi(p(s)) ds \\ & + \sigma_1 (G^{(1)} \otimes B_1)p(t) \\ & + \sigma_2 (G^{(2)} \otimes B_2)p(t-r(t)) \\ & + \sigma_3 (G^{(3)} \otimes B_3) \int_{t-d(t)}^t p(s) ds + Kp(t-\tau(t)) \\ & + (I_N \otimes E_1)\omega(t), \\ z(t) = & (I_N \otimes D_1)p(t) + (I_N \otimes D_2)p(t-r(t)) \\ & + (I_N \otimes E_2)\omega(t). \end{aligned} \quad (12)$$

So far the following definitions and lemmas are introduced to be served for the proof of the main results.

*Definition 1 [54]:* For given matrices  $F_1, F_2, F_3$ , and  $F_4$  satisfying Assumption 2, system (12) is said to be extended dissipative, if, under the zero initial condition, there exists a scalar  $\delta$  such that the following inequality holds for any  $t_f \geq 0$  and all  $\omega(t) \in \mathcal{L}_2[0, \infty)$ :

$$\int_0^{t_f} J(s) ds \geq \sup_{0 \leq t \leq t_f} z^T(t) F_4 z(t) + \delta, \quad (13)$$

where

$$J(s) = z^T(s) F_1 z(s) + 2z^T(s) F_2 \omega(s) + \omega^T(s) F_3 \omega(s). \quad (14)$$

*Remark 1:* The inequality (13) implies that the new performance contains more general solution by setting the weighting matrices  $F_i$ ,  $i = 1, 2, 3, 4$ , (i.e.)

- If  $F_1 = 0, F_2 = 0, F_3 = \gamma^2 I, F_4 = I$ , and  $\delta = 0$  then the inequality (13) becomes the  $L_2 - L_\infty$  performance;
- If  $F_1 = -I, F_2 = 0, F_3 = \gamma^2 I, F_4 = 0$ , and  $\delta = 0$  then the inequality (13) determines the  $H_\infty$  performance;
- If  $F_1 = 0, F_2 = I, F_3 = \gamma I, F_4 = 0$ , and  $\delta = 0$  then the inequality (13) reduces to the passivity performance;
- If  $F_1 = Q, F_2 = S, F_3 = R - \gamma I, F_4 = 0$ , and  $\delta = 0$  then the inequality (13) degenerates the  $(Q, S, R) - \gamma$ -dissipativity performance.

The following assumptions are made throughout this paper.

*Assumption 1:* The activation functions  $f_i(\cdot)$ ,  $i = 1, 2, \dots, n$ , satisfy Lipschitzian with the Lipschitz constants  $f_i > 0$ :

$$\|f_i(y(\theta)) - f_i(\alpha(t)w(\theta))\| \leq f_i \|y(\theta) - \alpha(t)w(\theta)\|,$$

where  $\Gamma$  is positive constant matrix and  $\Gamma = \text{diag}\{f_i, i = 1, 2, \dots, n\}$ .

*Assumption 2:* [54]: For given real symmetric matrices  $F_1 \leq 0, F_3, F_4 \geq 0$ , and a real matrix  $F_2$ , the following conditions are satisfied:

1.  $\|E_2\| \cdot \|F_4\| = 0$ ,
2.  $(\|F_1\| + \|F_2\|) \cdot \|F_4\| = 0$ ,
3.  $E_2^T F_1 E_2 + E_2^T F_2 + F_2^T E_2 + F_3 > 0$ .

*Lemma 1* ([62], Cauchy Inequality): For any symmetric positive definite matrix  $R \in \mathcal{R}^{n \times n}$  and  $x, y \in \mathcal{R}^n$  we have

$$\pm 2x^T y \leq x^T R x + y^T R^{-1} y.$$

*Lemma 2* [62]: For any constant symmetric matrix  $W \in \mathcal{R}^{m \times m}$ ,  $W = W^T > 0$ ,  $b > 0$ , vector function  $p : [0, b] \rightarrow \mathcal{R}^m$  such that the integrations concerned are well defined, one has

$$\left(\int_0^b p^T(s) ds\right)^T W \left(\int_0^b p(s) ds\right) \leq b \int_0^b p^T(s) W p(s) ds.$$

*Lemma 3* [63]: For a positive definite matrix  $S > 0$  and a function  $p : [a, b] \rightarrow \mathcal{R}^n$  whose derivative  $\dot{p} \in C([a, b], \mathcal{R}^n)$ , the following inequalities hold:

$$\begin{aligned} \int_a^b \dot{p}^T(s) S \dot{p}(s) ds &\geq \frac{1}{b-a} \Pi_1^T S \Pi_1 \\ &+ \frac{3}{b-a} \Pi_2^T S \Pi_2 \\ &+ \frac{5}{b-a} \Pi_3^T S \Pi_3 \\ &+ \frac{7}{b-a} \Pi_4^T S \Pi_4, \end{aligned}$$

$$\int_a^b \int_a^b \dot{p}^T(s) S \dot{p}(s) ds d\vartheta \geq 2\Pi_5^T S \Pi_5 + 4\Pi_6^T S \Pi_6,$$

where

$$\Pi_1 = p(b) - p(a),$$

$$\Pi_2 = p(b) + p(a) - \frac{2}{b-a} \int_a^b p(s) ds,$$

$$\begin{aligned} \Pi_3 &= p(b) - p(a) + \frac{6}{b-a} \int_a^b p(s) ds \\ &- \frac{12}{(b-a)^2} \int_a^b \int_a^b p(s) ds d\vartheta, \end{aligned}$$

$$\begin{aligned} \Pi_4 &= p(b) + p(a) - \frac{12}{b-a} \int_a^b p(s) ds \\ &+ \frac{60}{(b-a)^2} \int_a^b \int_a^b p(s) ds d\vartheta \\ &- \frac{120}{(b-a)^3} \int_a^b \int_a^b \int_a^b p(s) ds d\vartheta du, \end{aligned}$$

$$\Pi_5 = p(b) - \frac{1}{b-a} \int_a^b p(s) ds,$$

$$\begin{aligned} \Pi_6 &= p(b) + \frac{2}{b-a} \int_a^b p(s) ds \\ &- \frac{6}{(b-a)^2} \int_a^b \int_a^b p(s) ds d\vartheta. \end{aligned}$$

*Lemma 4* [64]: For any symmetric positive definite matrix  $\Lambda \in \mathcal{R}^{n \times n}$ ,  $M_1, M_2 \in \mathcal{R}^{m \times n}$ ,  $\Omega \in \mathcal{R}^{2n \times m}$ ,  $\forall \beta \in (0, 1)$ , the following inequality holds:

$$\begin{aligned} -\Omega^T \begin{bmatrix} \frac{1}{\beta} \Lambda & 0 \\ 0 & \frac{1}{1-\beta} \Lambda \end{bmatrix} \Omega \\ \leq -\Omega^T \Sigma(\beta) \Omega \\ -\text{sym} \left\{ \Omega^T \begin{bmatrix} (1-\beta)M_1^T \\ \beta M_2^T \end{bmatrix} \right\} + \beta M_1 \Lambda^{-1} M_1^T \\ + (1-\beta) M_2 \Lambda^{-1} M_2^T, \end{aligned}$$

where

$$\Sigma(\beta) = \begin{bmatrix} (2-\beta)\Lambda & 0 \\ 0 & (1+\beta)\Lambda \end{bmatrix}.$$

*Lemma 5* [64]: Consider a parameter dependent symmetric matrix  $\Psi(\beta) \in \mathcal{R}^{m \times m}$ , such that the convex inequality

$$\Psi(\beta) \leq (1-\beta)\Psi(0) + \beta\Psi(1),$$

holds for all  $\beta \in [0, 1]$ . If there exist a symmetric positive definite matrix  $\Lambda \in \mathcal{R}^{n \times n}$  and two matrices  $M_1, M_2 \in \mathcal{R}^{m \times n}$ , such that the inequality

$$\Upsilon(\beta) = \begin{bmatrix} \Omega & \beta M_1 + (1-\beta)M_2 \\ * & -\Lambda \end{bmatrix} < 0,$$

where

$$\Omega = \Psi(\beta) - \Omega^T \Sigma(\beta) \Omega - \text{sym} \left\{ \Omega^T \begin{bmatrix} (1-\beta)M_1^T \\ \beta M_2^T \end{bmatrix} \right\},$$

holds for  $\beta \in \{0, 1\}$ , then the following inequality holds:

$$\Psi(\beta) - \Omega^T \begin{bmatrix} \frac{1}{\beta} \Lambda & 0 \\ 0 & \frac{1}{1-\beta} \Lambda \end{bmatrix} \Omega < 0, \quad \forall \beta \in (0, 1).$$

*Lemma 6* ([62], Schur Complement Lemma): Given constant symmetric matrices  $P, Q, R$  with appropriate dimensions satisfying  $P = P^T, Q = Q^T > 0$ , one has  $P + R^T Q^{-1} R < 0$  if and only if

$$\begin{bmatrix} P & R^T \\ R & -Q \end{bmatrix} < 0 \quad \text{or} \quad \begin{bmatrix} -Q & R \\ R^T & P \end{bmatrix} < 0.$$

*Remark 2:* The merit of our method is that hybrid couplings are considered for the first time, which contain constant, discrete, and distributed delay couplings. These additional tools are more practical than the references in [10], [57], [58]. Moreover, we obtain new FPS with extended dissipative containing, passive, and dissipative performance. Additionally, the conditions are more general than those in [34]–[36], [39], [40], [43], [44], [57]–[59], and these couplings are not inputted. We can notice that their conditions cannot be simulated to our examples.

*Remark 3:* Differing from references [10], [11], [57], [58], we are first concerned with the FPS problem for NNs, including both discrete and distributed delays. Moreover, these delays are not necessarily differentiable functions that can be easily used in a real-world application which differ from [6], [22], [32]. For the first time, we obtained new FPS stability and extended dissipativity criteria that contain  $H_\infty$ ,  $L_2 - L_\infty$ , passivity, and dissipativity performance by setting parameters in the general formulation, which has not yet been reported for delayed coupled NNs. Additionally, we use mixed nonlinear and pinning sampled-data controls, which are unlike previous work [59]–[61].

### III. MAIN RESULTS

In this section, we present control scheme to synchronize the NNs (1) to the homogenous trajectory (3). Then, we will give some sufficient conditions in the FPS of NNs with mixed time-varying delays and hybrid coupling. Before proposing the main results, for the sake of presentation simplicity, we denote:

$$\begin{aligned} \mathcal{X}(t) &= \left[ p^T(t), p^T(t-r_1), p^T(t-r_2), p^T(t-r(t)), \right. \\ &\quad \dot{p}(t), p^T(t-\tau), p^T(t-\tau(t)), \eta_1(t), \eta_2(t), \\ &\quad \left. \eta_3(t), \eta_4(t) \right]^T, \\ \eta_1(t) &= \left[ \frac{1}{r_1} \int_{t-r_1}^t p^T(s) ds, \frac{1}{r(t)-r_1} \int_{t-r(t)}^{t-r_1} p^T(s) ds, \right. \\ &\quad \left. \frac{1}{r_2-r(t)} \int_{t-r_2}^{t-r(t)} p^T(s) ds \right]^T, \\ \eta_2(t) &= \left[ \frac{1}{r_1^2} \int_{t-r_1}^t \int_{\vartheta}^t p^T(s) dsd\vartheta, \right. \\ &\quad \frac{1}{(r(t)-r_1)^2} \int_{t-r(t)}^{t-r_1} \int_{\vartheta}^{t-r_1} p^T(s) dsd\vartheta, \\ &\quad \left. \frac{1}{(r_2-r(t))^2} \int_{t-r_2}^{t-r(t)} \int_{\vartheta}^{t-r(t)} p^T(s) dsd\vartheta \right]^T, \\ \eta_3(t) &= \left[ \frac{1}{r_1^3} \int_{t-r_1}^t \int_u^t \int_{\vartheta}^t p^T(s) dsd\vartheta du, \right. \\ &\quad \frac{1}{(r(t)-r_1)^3} \\ &\quad \times \int_{t-r(t)}^{t-r_1} \int_u^{t-r_1} \int_{\vartheta}^{t-r_1} p^T(s) dsd\vartheta du, \\ &\quad \left. \frac{1}{(r_2-r(t))^3} \right. \\ &\quad \times \left. \int_{t-r_2}^{t-r(t)} \int_u^{t-r(t)} \int_{\vartheta}^{t-r(t)} p^T(s) dsd\vartheta du \right]^T, \\ \eta_4(t) &= \left[ \int_{t-d(t)}^t p^T(s) ds, \omega(t) \right]^T, \end{aligned} \quad (15)$$

where  $v_i \in \mathcal{R}^{n \times 18n}$  is defined as  $v_i = [0_{n \times (i-1)n}, I_n, 0_{n \times (18-i)n}]$  for  $i = 1, 2, \dots, 18$ .

### A. SYNCHRONIZATION ANALYSIS WITH SAMPLE-DATA CONTROL

The following stability theorem is given for system (12) with  $\omega(t) = 0$ .

*Theorem 1:* For given scalars  $r_1, r_2, d$  and  $\tau$  if there exist real positive matrices  $P \in \mathcal{R}^{5n \times 5n}$ ,  $Q_0, S_0, Q_i, S_k, R_1, R_2 \in \mathcal{R}^{n \times n}$  ( $i = 1, 2, 3, 4; k = 1, 2, 3$ ),  $M_1, M_2 \in \mathcal{R}^{17n \times 4n}$ , positive constants  $\epsilon_i$  ( $i = 1, 2, \dots, 6$ ), and any matrices  $Y = \text{diag}\{Y_1, Y_2, \dots, Y_N\}$ ,  $Z = \text{diag}\{Z_1, Z_2, \dots, Z_N\}$  with appropriate dimensions, such that the following hold:

$$\Upsilon(\beta) = \begin{bmatrix} \Upsilon_{11} & \beta M_1 + (1-\beta)M_2 & \tilde{\Upsilon}_{13} \\ * & -\Lambda & 0 \\ * & * & \tilde{\Upsilon}_{33} \end{bmatrix} < 0, \quad (16)$$

for  $\beta = \{0, 1\}$ , where

$$\begin{aligned} \tilde{\Upsilon}_{13} &= [\Upsilon_{13} \ \Upsilon_{14} \ \Upsilon_{15} \ \Upsilon_{16} \ \Upsilon_{17} \ \Upsilon_{18}], \\ \tilde{\Upsilon}_{33} &= \text{diag}\left\{-\frac{\epsilon_1}{2}I, -\frac{\epsilon_2}{2}I, -\frac{\epsilon_3}{2}I, -\frac{\epsilon_4}{2}I, -\frac{\epsilon_5}{2}I, -\frac{\epsilon_6}{2}I\right\}, \end{aligned}$$

$$\begin{aligned} \Upsilon_{11} &= \sum_{i=1}^5 \Pi_i - \Omega^T \Sigma(\beta) \Omega \\ &\quad - \text{sym} \left\{ \Omega^T \begin{bmatrix} (1-\beta)M_1^T \\ \beta M_2^T \end{bmatrix} \right\}, \end{aligned}$$

$$\Upsilon_{13} = I_N \otimes ZA_1, \quad \Upsilon_{14} = I_N \otimes ZA_2,$$

$$\Upsilon_{15} = I_N \otimes ZA_3, \quad \Upsilon_{16} = I_N \otimes ZA_1,$$

$$\Upsilon_{17} = I_N \otimes ZA_2, \quad \Upsilon_{18} = I_N \otimes ZA_3,$$

$$\begin{aligned} \Pi_1 &= \Theta_1^T P \Theta_2 + \Theta_2^T P \Theta_1 - \Theta_3^T S_0 \Theta_3 - \Theta_4^T S_0 \Theta_4 \\ &\quad + \tau v_5^T S_0 v_5 + v_1^T Q_0 v_1 - v_6^T Q_0 v_6, \end{aligned}$$

$$\begin{aligned} \Pi_2 &= v_1^T (Q_1 + \Gamma^T Q_2 \Gamma) v_1 - v_2^T (Q_1 + \Gamma^T Q_2 \Gamma) v_2 \\ &\quad + v_2^T (Q_3 + \Gamma^T Q_4 \Gamma) v_2 \\ &\quad - v_3^T (Q_3 + \Gamma^T Q_4 \Gamma) v_3, \end{aligned}$$

$$\begin{aligned} \Pi_3 &= v_5^T (r_1^2 S_1 + r_2^2 S_2) v_5 + d^2 v_1^T \Gamma^T S_3 \Gamma v_1 \\ &\quad - v_{17}^T \Gamma^T S_3 \Gamma v_{17} - \Theta_5^T S_1 \Theta_5 - 3\Theta_6^T S_1 \Theta_6 \\ &\quad - 5\Theta_7^T S_1 \Theta_7 - 7\Theta_8^T S_1 \Theta_8, \end{aligned}$$

$$\begin{aligned} \Pi_4 &= -2\Theta_{17}^T R_1 \Theta_{17} - 4\Theta_{18}^T R_1 \Theta_{18} - 2\Theta_{19}^T R_2 \Theta_{19} \\ &\quad - 4\Theta_{20}^T R_2 \Theta_{20} - 2\Theta_{21}^T R_2 \Theta_{21} - 4\Theta_{22}^T R_2 \Theta_{22}, \end{aligned}$$

$$\begin{aligned} \Pi_5 &= v_1^T Z S_0 + S_0^T Z^T v_1 + v_5^T Z S_0 + S_0^T Z^T v_5 \\ &\quad + v_1^T Y v_4 + v_4^T Y^T v_1 + v_5^T Y v_4 + v_4^T Y^T v_5, \\ &\quad + \frac{1}{2}(\epsilon_1 + \epsilon_4) v_1^T (I_N \otimes \Gamma^T \Gamma) v_1 \\ &\quad + \frac{1}{2}(\epsilon_2 + \epsilon_5) v_4^T (I_N \otimes \Gamma^T \Gamma) v_4 \\ &\quad + \frac{1}{2}(\epsilon_3 + \epsilon_6) v_{17}^T (I_N \otimes \Gamma^T \Gamma) v_{17}, \end{aligned}$$

$$S_0 = [\sigma_1(G^{(1)} \otimes B_1) - (I_N \otimes C)] v_1$$

$$+ \sigma_2(G^{(2)} \otimes B_2) v_4$$

$$+ \sigma_3(G^{(3)} \otimes B_3) v_{17} - v_5,$$

$$\Lambda = \text{diag}\{S_2, 3S_2, 5S_2, 7S_2\},$$

$$\Omega = \left[ \Theta_9^T \ \Theta_{10}^T \ \Theta_{11}^T \ \Theta_{12}^T \ \Theta_{13}^T \ \Theta_{14}^T \ \Theta_{15}^T \ \Theta_{16}^T \right]^T, \quad (17)$$

with

$$\begin{aligned} \Theta_1 &= [v_1^T, r_1 v_8^T, \beta r_{21} v_9^T - (1 - \beta) r_{21} v_{10}^T, \\ &\quad r_1^2 v_{11}^T, r_1^3 v_{14}^T]^T, \\ \Theta_2 &= [v_5^T, v_1^T - v_2^T, v_2^T - v_3^T, r_1 v_1^T - r_1 v_8^T, \\ &\quad \frac{1}{2} r_1^2 v_1^T - r_1^2 v_{11}^T]^T, \\ \Theta_3 &= v_1 - v_7, \quad \Theta_4 = v_7 - v_6, \\ \Theta_5 &= v_1 - v_2, \quad \Theta_6 = v_1 + v_2 - 2v_8, \\ \Theta_7 &= v_1 - v_2 + 6v_8 - 12v_{11}, \\ \Theta_8 &= v_1 + v_2 - 12v_8 + 60v_{11} - 1200v_{14}, \\ \Theta_9 &= v_2 - v_4, \quad \Theta_{10} = v_2 + v_4 - 2v_9, \\ \Theta_{11} &= v_2 - v_4 + 6v_9 - 12v_{12}, \\ \Theta_{12} &= v_2 + v_4 - 12v_9 + 60v_{12} - 1200v_{15}, \\ \Theta_{13} &= v_4 - v_3, \quad \Theta_{14} = v_4 + v_3 - 2v_{10}, \\ \Theta_{15} &= v_4 - v_3 + 6v_{10} - 12v_{13}, \\ \Theta_{16} &= v_4 + v_3 - 12v_{10} + 60v_{13} - 1200v_{16}, \\ \Theta_{17} &= v_1 - v_8, \quad \Theta_{18} = v_1 + 2v_8 - 6v_{11}, \\ \Theta_{19} &= v_2 - v_9, \quad \Theta_{20} = v_2 + 2v_9 - 6v_{12}, \\ \Theta_{21} &= v_4 - v_{10}, \quad \Theta_{22} = v_4 + 2v_{10} - 6v_{13}, \end{aligned}$$

then, the system (12) with  $\omega(t) = 0$  is asymptotically stable with the gained sampled-data feedback controller designed as  $K = Z^{-1}Y$ .

*Proof:* We consider a candidate Lyapunov-Krasovskii functional:

$$V(p(t), t) = \sum_{i=1}^4 V_i(p(t), t), \quad (18)$$

where

$$\begin{aligned} V_1(p(t), t) &= \mathcal{P}^T(t) P \mathcal{P}(t) + \int_{t-\tau}^t p^T(s) Q_0 p(s) ds \\ &\quad + \int_{t-\tau}^t \int_{\vartheta}^t \dot{p}^T(s) S_0 \dot{p}(s) ds d\vartheta, \\ V_2(p(t), t) &= \int_{t-r_1}^t [p^T(s) Q_1 p(s) \\ &\quad + f^T(p(s)) Q_2 f(p(s))] ds \\ &\quad + \int_{t-r_2}^{t-r_1} [p^T(s) Q_3 p(s) \\ &\quad + f^T(p(s)) Q_4 f(p(s))] ds, \\ V_3(p(t), t) &= r_1 \int_{t-r_1}^t \int_{\vartheta}^t \dot{p}^T(s) S_1 \dot{p}(s) ds d\vartheta \\ &\quad + r_{21} \int_{t-r_2}^{t-r_1} \int_{\vartheta}^t \dot{p}^T(s) S_2 \dot{p}(s) ds d\vartheta \\ &\quad + d \int_{t-d}^t \int_{\vartheta}^t f^T(p(s)) S_3 f(p(s)) ds d\vartheta, \\ V_4(p(t), t) &= \int_{t-r_1}^t \int_{\varphi}^t \int_{\vartheta}^t \dot{p}^T(s) R_1 \dot{p}(s) ds d\vartheta d\varphi \end{aligned}$$

$$+ \int_{-r_2}^{t-r_1} \int_{\varphi}^{t-r_1} \int_{t+\vartheta}^t \dot{p}^T(s) R_2 \dot{p}(s) ds d\vartheta d\varphi,$$

where

$$\begin{aligned} \mathcal{P}(t) &= \left[ p^T(t), \int_{t-r_1}^t p^T(s) ds, \int_{t-r_2}^{t-r_1} p^T(s) ds, \right. \\ &\quad \left. \int_{t-r_1}^t \int_{\vartheta}^t p^T(s) ds d\vartheta, \int_{t-r_1}^t \int_{\varphi}^t \int_{\vartheta}^t p^T(s) ds d\vartheta d\varphi \right]^T. \end{aligned}$$

By taking the derivative of  $V(p(t), t)$  along the trajectories of the error system (12), we get

$$\begin{aligned} \dot{V}_1(p(t), t) &= 2\dot{\mathcal{P}}^T(t) P \mathcal{P}(t) + p^T(t) Q_0 p(t) \\ &\quad - p^T(t - \tau) Q_0 p(t - \tau) + \tau \dot{p}^T(t) S_0 \dot{p}(t) \\ &\quad - \tau \int_{t-\tau}^t \dot{p}^T(s) S_0 \dot{p}(s) ds, \quad (19) \end{aligned}$$

$$\begin{aligned} \dot{V}_2(p(t), t) &= p^T(t) Q_1 p(t) + f^T(p(t)) Q_2 f(p(t)) \\ &\quad - p^T(t - r_1) Q_1 p(t - r_1) \\ &\quad - f^T(p(t - r_1)) Q_2 f(p(t - r_1)) \\ &\quad + p^T(t - r_1) Q_3 p(t - r_1) \\ &\quad + f^T(p(t - r_1)) Q_4 f(p(t - r_1)) \\ &\quad - p^T(t - r_2) Q_3 p(t - r_2) \\ &\quad - f^T(p(t - r_2)) Q_4 f(p(t - r_2)), \\ &\leq p^T(t) (Q_1 + \Gamma^T Q_2 \Gamma) p(t) \\ &\quad - p^T(t - r_1) (Q_1 + \Gamma^T Q_2 \Gamma) p(t - r_1) \\ &\quad + p^T(t - r_1) (Q_3 + \Gamma^T Q_4 \Gamma) p(t - r_1) \\ &\quad - p^T(t - r_2) (Q_3 + \Gamma^T Q_4 \Gamma) p(t - r_2), \\ &= \mathcal{X}^T(t) \Pi_2 \mathcal{X}(t), \quad (20) \end{aligned}$$

$$\begin{aligned} \dot{V}_3(p(t), t) &= r_1^2 \dot{p}^T(t) S_1 \dot{p}(t) - r_1 \int_{t-r_1}^t \dot{p}^T(s) S_1 \dot{p}(s) ds \\ &\quad + r_{21}^2 \dot{p}^T(t) S_2 \dot{p}(t) \\ &\quad - r_{21} \int_{t-r_2}^{t-r_1} \dot{p}^T(s) S_2 \dot{p}(s) ds \\ &\quad + d^2 f^T(p(t)) S_3 f(p(t)) \\ &\quad - d \int_{t-d}^t f^T(p(s)) S_3 f(p(s)) ds, \\ &\leq \dot{p}^T(t) (r_1^2 S_1 + r_{21}^2 S_2) \dot{p}(t) \\ &\quad + d^2 p(t) \Gamma^T S_3 \Gamma p(t) \\ &\quad - r_1 \int_{t-r_1}^t \dot{p}^T(s) S_1 \dot{p}(s) ds \\ &\quad - r_{21} \int_{t-r_2}^{t-r_1} \dot{p}^T(s) S_2 \dot{p}(s) ds \\ &\quad - d \int_{t-d}^t f^T(p(s)) S_3 f(p(s)) ds, \quad (21) \end{aligned}$$

$$\begin{aligned} \dot{V}_4(p(t), t) &= \frac{r_1^2}{2} \dot{p}^T(t) R_1 \dot{p}(t) + \frac{r_{21}^2}{2} \dot{p}^T(t) R_2 \dot{p}(t) \\ &\quad - \int_{t-r_1}^t \int_{\vartheta}^t \dot{p}^T(s) R_1 \dot{p}(s) ds d\vartheta \\ &\quad - \int_{-r_2}^{t-r_1} \int_{t+\vartheta}^{t-r_1} \dot{p}^T(s) R_2 \dot{p}(s) ds d\vartheta, \quad (22) \end{aligned}$$

where  $\Pi_2$  is defined in (17). Applying Lemma 2 and Lemma 3, it can be shown that

$$\begin{aligned}
 & -\tau \int_{t-\tau}^t \dot{p}^T(s) S_0 \dot{p}(s) ds \\
 & = -\tau \int_{t-\tau(t)}^t \dot{p}^T(s) S_0 \dot{p}(s) ds \\
 & \quad -\tau \int_{t-\tau}^{t-\tau(t)} \dot{p}^T(s) S_0 \dot{p}(s) ds, \\
 & \leq -\left[p(t) - p(t - \tau(t))\right]^T S_0 \left[p(t) - p(t - \tau(t))\right] \\
 & \quad -\left[p(t - \tau(t)) - p(t - \tau)\right]^T S_0 \\
 & \quad \times \left[p(t - \tau(t)) - p(t - \tau)\right]. \tag{23}
 \end{aligned}$$

$$\begin{aligned}
 & -r_1 \int_{t-r_1}^t \dot{p}^T(s) S_1 \dot{p}(s) ds \\
 & \leq -\Theta_5^T S_1 \Theta_5 - 3\Theta_6^T S_1 \Theta_6 - 5\Theta_7^T S_1 \Theta_7 \\
 & \quad -7\Theta_8^T S_1 \Theta_8. \tag{24}
 \end{aligned}$$

$$\begin{aligned}
 & -d \int_{t-d}^t f^T(p(s)) S_3 f(p(s)) ds \\
 & \leq -d \int_{t-d(t)}^t f^T(p(s)) S_3 f(p(s)) ds, \\
 & \leq -\int_{t-d(t)}^t f^T(p(s)) ds S_3 \int_{t-d(t)}^t f(p(s)) ds, \\
 & \leq -\int_{t-d(t)}^t p^T(s) ds \left(\Gamma^T S_3 \Gamma\right) \int_{t-d(t)}^t p(s) ds. \tag{25}
 \end{aligned}$$

$$\begin{aligned}
 & -\int_{t-r_1}^t \int_{\vartheta}^t \dot{p}^T(s) R_1 \dot{p}(s) ds d\vartheta \\
 & \quad -\int_{t-r_2}^{t-r_1} \int_{\vartheta}^{t-r_1} \dot{p}^T(s) R_2 \dot{p}(s) ds d\vartheta \\
 & \leq \mathcal{X}^T(t) \Pi_4 \mathcal{X}(t). \tag{26}
 \end{aligned}$$

Let  $\beta = \frac{r(t)-r_1}{r_{21}}$ , and applying the auxiliary function-based inequality, Lemma 4 and Lemma 5 yields

$$\begin{aligned}
 & -r_{21} \int_{t-r_2}^{t-r_1} \dot{p}^T(s) S_2 \dot{p}(s) ds \\
 & = -r_{21} \int_{t-r(t)}^{t-r_1} \dot{p}^T(s) S_2 \dot{p}(s) ds \\
 & \quad -r_{21} \int_{t-r_2}^{t-r(t)} \dot{p}^T(s) S_2 \dot{p}(s) ds, \\
 & \leq -\frac{r_{21}}{r(t) - r_1} (\Theta_9^T S_2 \Theta_9 + 3\Theta_{10}^T S_2 \Theta_{10} + 5\Theta_{11}^T S_2 \Theta_{11} \\
 & \quad + 7\Theta_{12}^T S_2 \Theta_{12}) \\
 & \quad -\frac{r_{21}}{r_2 - r(t)} (\Theta_{13}^T S_2 \Theta_{13} + 3\Theta_{14}^T S_2 \Theta_{14} + 5\Theta_{15}^T S_2 \Theta_{15} \\
 & \quad + 7\Theta_{16}^T S_2 \Theta_{16}), \\
 & = -\frac{1}{\beta} (\Theta_9^T S_2 \Theta_9 + 3\Theta_{10}^T S_2 \Theta_{10} + 5\Theta_{11}^T S_2 \Theta_{11} \\
 & \quad + 7\Theta_{12}^T S_2 \Theta_{12})
 \end{aligned}$$

$$\begin{aligned}
 & -\frac{1}{1-\beta} (\Theta_{13}^T S_2 \Theta_{13} + 3\Theta_{14}^T S_2 \Theta_{14} + 5\Theta_{15}^T S_2 \Theta_{15} \\
 & \quad + 7\Theta_{16}^T S_2 \Theta_{16}), \\
 & = -\Omega^T \begin{bmatrix} \frac{1}{\beta} \Lambda & 0 \\ 0 & \frac{1}{1-\beta} \Lambda \end{bmatrix} \Omega, \\
 & \leq -\Omega^T \Sigma(\beta) \Omega - \text{sym} \left\{ \Omega^T \begin{bmatrix} (1-\beta)M_1^T \\ \beta M_2^T \end{bmatrix} \right\} \\
 & \quad + \beta M_1 \Lambda^{-1} M_1^T + (1-\beta) M_2 \Lambda^{-1} M_2^T, \tag{27}
 \end{aligned}$$

where  $M_1, M_2 \in \mathcal{R}^{17n \times 4n}$ ,  $\Lambda = \text{diag}\{S_2, 3S_2, 5S_2, 7S_2\}$ ,  $\Omega = \left[\Theta_9^T \ \Theta_{10}^T \ \Theta_{11}^T \ \Theta_{12}^T \ \Theta_{13}^T \ \Theta_{14}^T \ \Theta_{15}^T \ \Theta_{16}^T\right]^T$  and

$$\Sigma(\beta) = \begin{bmatrix} (2-\beta)\Lambda & 0 \\ 0 & (1+\beta)\Lambda \end{bmatrix}.$$

On the other hand, we consider the following zero equation:

$$\begin{aligned}
 0 & = 2\left[p^T(t) + \dot{p}^T(t)\right] Z \left[-(I_N \otimes C)p(t) \right. \\
 & \quad + (I_N \otimes A_1)\xi(p(t)) + (I_N \otimes A_2)\xi(p(t-r(t))) \\
 & \quad + (I_N \otimes A_3) \int_{t-d(t)}^t \xi(p(s)) ds + \sigma_1(G^{(1)} \otimes B_1)p(t) \\
 & \quad + \sigma_2(G^{(2)} \otimes B_2)p(t-r(t)) + \sigma_3(G^{(3)} \otimes B_3) \\
 & \quad \left. \times \int_{t-d(t)}^t p(s) ds + Kp(t-\tau(t)) - \dot{p}(t)\right]. \tag{28}
 \end{aligned}$$

Applying Lemma 1 and Lemma 2, we have

$$\begin{aligned}
 & p^T(t)(I_N \otimes ZA_1)\xi(p(t)) \\
 & \leq \frac{1}{2\epsilon_1} p^T(t)(I_N \otimes ZA_1 A_1^T Z^T)p(t) \\
 & \quad + \frac{\epsilon_1}{2} \xi^T(p(t))(I_N \otimes I_n)\xi(p(t)), \\
 & \leq \frac{1}{2\epsilon_1} p^T(t)(I_N \otimes ZA_1 A_1^T Z^T)p(t) \\
 & \quad + \frac{\epsilon_1}{2} p^T(t)(I_N \otimes \Gamma^T \Gamma)p(t), \\
 & = \frac{1}{2} p^T(t)(I_N \otimes ZA_1)\epsilon_1^{-1}(I_N \otimes A_1^T Z^T)p(t) \\
 & \quad + \frac{\epsilon_1}{2} p^T(t)(I_N \otimes \Gamma^T \Gamma)p(t), \tag{29} \\
 & p^T(t)(I_N \otimes ZA_2)\xi(p(t-r(t))) \\
 & \leq \frac{1}{2\epsilon_2} p^T(t)(I_N \otimes ZA_2 A_2^T Z^T)p(t) \\
 & \quad + \frac{\epsilon_2}{2} \xi^T((t-r(t)))(I_N \otimes I_n)\xi(p(t-r(t))), \\
 & \leq \frac{1}{2\epsilon_2} p^T(t)(I_N \otimes ZA_2 A_2^T Z^T)p(t) \\
 & \quad + \frac{\epsilon_2}{2} p^T(t-r(t))(I_N \otimes \Gamma^T \Gamma)p(t-r(t)), \\
 & = \frac{1}{2} p^T(t)(I_N \otimes ZA_2)\epsilon_2^{-1}(I_N \otimes A_2^T Z^T)p(t) \\
 & \quad + \frac{\epsilon_2}{2} p^T(t-r(t))(I_N \otimes \Gamma^T \Gamma)p(t-r(t)), \tag{30} \\
 & p^T(t)(I_N \otimes ZA_3) \int_{t-d(t)}^t \xi(p(s)) ds
 \end{aligned}$$



$$\begin{aligned}
 &\leq \frac{1}{2\epsilon_3} p^T(t)(I_N \otimes ZA_3 A_3^T Z^T) p(t) \\
 &\quad + \frac{\epsilon_3}{2} \left( \int_{t-d(t)}^t \xi^T(p(s)) ds \right)^T (I_N \otimes I_n) \\
 &\quad \times \left( \int_{t-d(t)}^t \xi(p(s)) ds \right), \\
 &\leq \frac{1}{2\epsilon_3} p^T(t)(I_N \otimes ZA_3 A_3^T Z^T) p(t) \\
 &\quad + \frac{\epsilon_3}{2} \left( \int_{t-d(t)}^t p^T(s) ds \right)^T (I_N \otimes \Gamma^T \Gamma) \left( \int_{t-d(t)}^t p(s) ds \right), \\
 &= \frac{1}{2} p^T(t)(I_N \otimes ZA_3) \epsilon_3^{-1} (I_N \otimes A_3^T Z^T) p(t) \\
 &\quad + \frac{\epsilon_3}{2} \left( \int_{t-d(t)}^t p^T(s) ds \right)^T (I_N \otimes \Gamma^T \Gamma) \\
 &\quad \times \left( \int_{t-d(t)}^t p(s) ds \right), \tag{31}
 \end{aligned}$$

$$\begin{aligned}
 &\dot{p}^T(t)(I_N \otimes ZA_1) \xi(p(t)) \\
 &\leq \frac{1}{2\epsilon_4} \dot{p}^T(t)(I_N \otimes ZA_1 A_1^T Z^T) \dot{p}(t) \\
 &\quad + \frac{\epsilon_4}{2} \xi^T(p(t))(I_N \otimes I_n) \xi(p(t)), \\
 &\leq \frac{1}{2\epsilon_4} \dot{p}^T(t)(I_N \otimes ZA_1 A_1^T Z^T) \dot{p}(t) \\
 &\quad + \frac{\epsilon_4}{2} p^T(t)(I_N \otimes \Gamma^T \Gamma) p(t), \\
 &= \frac{1}{2} \dot{p}^T(t)(I_N \otimes ZA_1) \epsilon_4^{-1} (I_N \otimes A_1^T Z^T) \dot{p}(t) \\
 &\quad + \frac{\epsilon_4}{2} p^T(t)(I_N \otimes \Gamma^T \Gamma) p(t), \tag{32}
 \end{aligned}$$

$$\begin{aligned}
 &\dot{p}^T(t)(I_N \otimes ZA_2) \xi(p(t-r(t))) \\
 &\leq \frac{1}{2\epsilon_5} \dot{p}^T(t)(I_N \otimes ZA_2 A_2^T Z^T) \dot{p}(t) \\
 &\quad + \frac{\epsilon_5}{2} \xi^T((t-r(t)))(I_N \otimes I_n) \xi(p(t-r(t))), \\
 &\leq \frac{1}{2\epsilon_5} \dot{p}^T(t)(I_N \otimes ZA_2 A_2^T Z^T) \dot{p}(t) \\
 &\quad + \frac{\epsilon_5}{2} p^T(t-r(t))(I_N \otimes \Gamma^T \Gamma) p(t-r(t)), \\
 &= \frac{1}{2} \dot{p}^T(t)(I_N \otimes ZA_2) \epsilon_5^{-1} (I_N \otimes A_2^T Z^T) \dot{p}(t) \\
 &\quad + \frac{\epsilon_5}{2} p^T(t-r(t))(I_N \otimes \Gamma^T \Gamma) p(t-r(t)), \tag{33}
 \end{aligned}$$

$$\begin{aligned}
 &\dot{p}^T(t)(I_N \otimes ZA_3) \int_{t-d(t)}^t \xi(p(s)) ds \\
 &\leq \frac{1}{2\epsilon_6} \dot{p}^T(t)(I_N \otimes ZA_3 A_3^T Z^T) \dot{p}(t) \\
 &\quad + \frac{\epsilon_6}{2} \left( \int_{t-d(t)}^t \xi^T(p(s)) ds \right)^T (I_N \otimes I_n) \\
 &\quad \times \left( \int_{t-d(t)}^t \xi(p(s)) ds \right), \\
 &\leq \frac{1}{2\epsilon_6} \dot{p}^T(t)(I_N \otimes ZA_3 A_3^T Z^T) \dot{p}(t)
 \end{aligned}$$

$$\begin{aligned}
 &\quad + \frac{\epsilon_6}{2} \left( \int_{t-d(t)}^t p^T(s) ds \right)^T (I_N \otimes \Gamma^T \Gamma) \left( \int_{t-d(t)}^t p(s) ds \right), \\
 &= \frac{1}{2} \dot{p}^T(t)(I_N \otimes ZA_3) \epsilon_6^{-1} (I_N \otimes A_3^T Z^T) \dot{p}(t) \\
 &\quad + \frac{\epsilon_6}{2} \left( \int_{t-d(t)}^t p^T(s) ds \right)^T (I_N \otimes \Gamma^T \Gamma) \\
 &\quad \times \left( \int_{t-d(t)}^t p(s) ds \right). \tag{34}
 \end{aligned}$$

Then, from  $\dot{V}(p(t), t)$ , and (23)-(34), can be estimated as

$$\begin{aligned}
 &\dot{V}(p(t), t) \\
 &\leq \mathcal{X}^T(t) \left\{ \sum_{i=1}^5 \Pi_i - \Omega^T \Sigma(\beta) \Omega \right. \\
 &\quad \left. - \text{sym} \left\{ \Omega^T \begin{bmatrix} (1-\beta)M_1^T \\ \beta M_2^T \end{bmatrix} \right\} + \beta M_1 \Lambda^{-1} M_1^T \right. \\
 &\quad \left. + (1-\beta)M_2 \Lambda^{-1} M_2^T + \frac{1}{2} v_1^T \Xi_1 v_1 + \frac{1}{2} v_5^T \Xi_2 v_5 \right\} \mathcal{X}(t), \tag{35}
 \end{aligned}$$

where  $\Pi_i$ , ( $i = 1, 2, \dots, 5$ ) are defined in (17) and

$$\begin{aligned}
 \Xi_1 &= (I_N \otimes ZA_1) \epsilon_1^{-1} (I_N \otimes A_1^T Z^T) \\
 &\quad + (I_N \otimes ZA_2) \epsilon_2^{-1} (I_N \otimes A_2^T Z^T) \\
 &\quad + (I_N \otimes ZA_3) \epsilon_3^{-1} (I_N \otimes A_3^T Z^T), \\
 \Xi_2 &= (I_N \otimes ZA_1) \epsilon_4^{-1} (I_N \otimes A_1^T Z^T) \\
 &\quad + (I_N \otimes ZA_2) \epsilon_5^{-1} (I_N \otimes A_2^T Z^T) \\
 &\quad + (I_N \otimes ZA_3) \epsilon_6^{-1} (I_N \otimes A_3^T Z^T).
 \end{aligned}$$

Applying the Schur complement of Lemma 6, we have

$$\dot{V}(p(t), t) \leq \mathcal{X}^T(t) \Upsilon(\beta) \mathcal{X}(t), \tag{36}$$

where  $\Upsilon(\beta)$  is defined in (16).

According to Lemma 4, if LMI (16) is verified for  $\beta = \{0, 1\}$ , then the inequality  $\Upsilon(\beta) < 0$  holds for all  $\beta \in (0, 1)$ . Then, the system (12) with  $\omega(t) = 0$  is asymptotically stable. This completes the proof.  $\square$

*Remark 4:* The FPS of NNs is implemented to mixed control in Theorem 1 where  $u_{i1}(t)$  is a nonlinear control (not pinning sampled-data control) and must be applied to each node. Relying on the pinning sampled-data control principle,  $u_{i2}(t)$  is a pinning sampled-data control intended to apply to the first  $l$  nodes  $0 \leq i \leq l$ . The selected or unselected pinning nodes don't base on the estimation of node errors, where one avoids rearranging each node errors. For further study, there is another technique which doesn't base on the estimation of node errors in the reference [65].

*Remark 5:* It is worth noting that sampled-data control has recently received much attention [33]–[36]. Because computation and communication resources are frequently limited in sampled-data implementation, reducing the data transmission load when using a sampled-data controller to achieve stability is critical. Furthermore, a neural network is typically composed of many high-dimensional nodes,

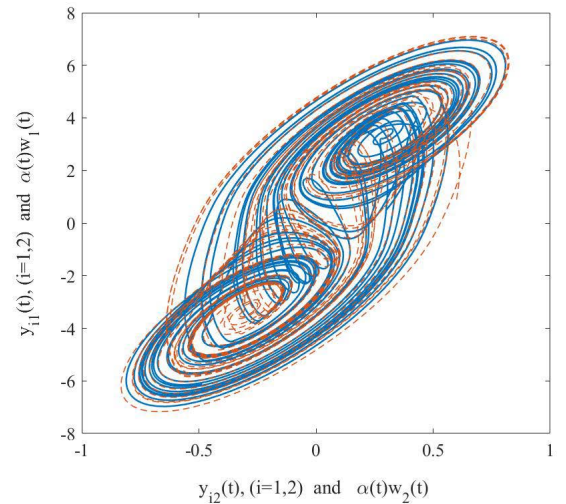
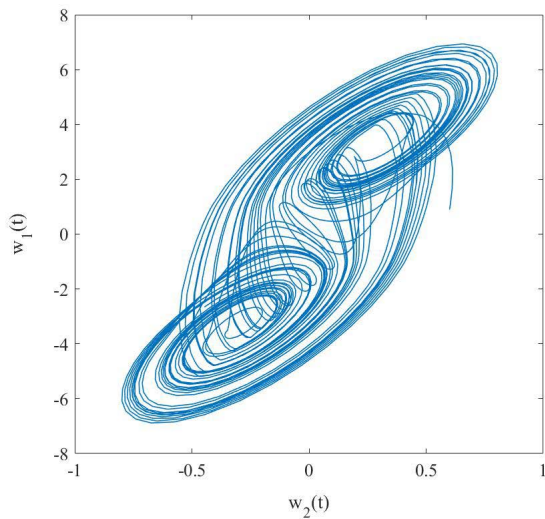
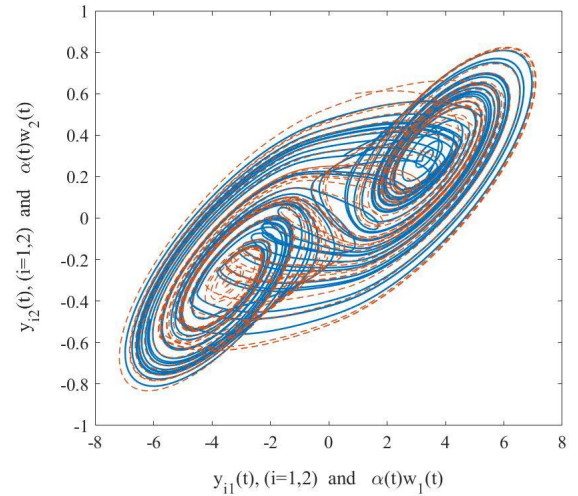
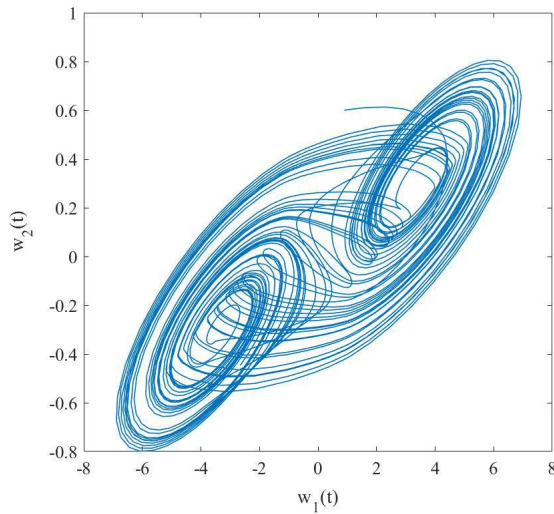


FIGURE 1. The trajectory of the isolated node (48) in Example 1.

FIGURE 2. The chaotic behavior of the network  $y_i(t)$  and the isolate node  $\alpha(t)w(t)$  in Example 1.

and controlling all neurons is expensive and impractical. To address this issue, we introduce pinning control, which allows us to control a subset of all nodes. Thus, the benefits of using pinning sampled-data control include low control equipment costs, reliability, and ease of application.

**B. EXTENDED DISSIPATIVE ANALYSIS WITH SAMPLE-DATA CONTROL**

For any non zero  $\omega(t) \in \mathcal{L}_2[0, \infty)$ , the extended dissipativity theorem can be obtained under the condition of assumption.

*Theorem 2:* For given scalars  $r_1, r_2, d, \tau$  and a positive scalar  $\kappa < 1$ , if there exist real positive matrices  $P \in \mathcal{R}^{5n \times 5n}$ ,  $Q_0, S_0, Q_i, S_k, R_1, R_2 \in \mathcal{R}^{n \times n}$  ( $i = 1, 2, 3, 4; k = 1, 2, 3$ ),  $M_1, M_2 \in \mathcal{R}^{18n \times 4n}$ , positive constants  $\epsilon_i$  ( $i = 1, 2, \dots, 6$ ), and any matrices  $Y = \text{diag}\{Y_1, Y_2, \dots, Y_N\}$ ,  $Z = \text{diag}\{Z_1, Z_2, \dots, Z_N\}$  with appropriate dimensions, such

that the following holds:

$$\tilde{\Upsilon}(\beta) = \begin{bmatrix} \Upsilon_{11} & \beta M_1 + (1 - \beta)M_2 & \tilde{\Upsilon}_{13} \\ * & -\Lambda & 0 \\ * & * & \tilde{\Upsilon}_{33} \end{bmatrix} < 0, \quad (37)$$

$$\begin{bmatrix} \kappa P - D_1^T F_4 D_1 & -D_1^T F_4 D_2 \\ * & (1 - \kappa)P - D_2^T F_4 D_2 \end{bmatrix} \geq 0, \quad (38)$$

for  $\beta = \{0, 1\}$ , where

$$\begin{aligned} \tilde{\Upsilon}_{11} &= \sum_{i=1}^4 \Pi_i + \bar{\Pi}_5 + \bar{\Pi}_6 - \Omega^T \Sigma(\beta) \Omega \\ &\quad - \text{sym} \left\{ \Omega^T \begin{bmatrix} (1 - \beta)M_1^T \\ \beta M_2^T \end{bmatrix} \right\}, \\ \bar{\Pi}_5 &= v_1^T Z \bar{S}_0 + \bar{S}_0^T Z^T v_1 + v_5^T Z \bar{S}_0 + \bar{S}_0^T Z^T v_5 \\ &\quad + v_1^T Y v_4 + v_4^T Y^T v_1 + v_5^T Y v_4 + v_4^T Y^T v_5, \end{aligned}$$

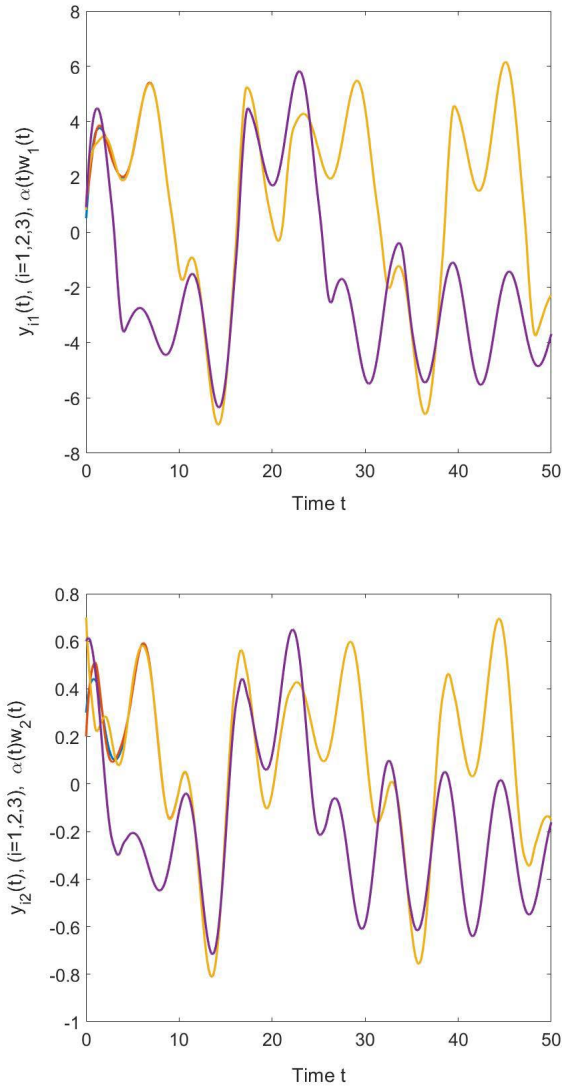


FIGURE 3. The state trajectories of the network  $y_i(t)$ , ( $i = 1, 2, 3$ ) and the isolate node  $\alpha(t)w(t)$  in Example 1.

$$\begin{aligned}
 & + \frac{1}{2}(\epsilon_1 + \epsilon_4)v_1^T(I_N \otimes \Gamma^T \Gamma)v_1 \\
 & + \frac{1}{2}(\epsilon_2 + \epsilon_5)v_4^T(I_N \otimes \Gamma^T \Gamma)v_4 \\
 & + \frac{1}{2}(\epsilon_3 + \epsilon_6)v_{17}^T(I_N \otimes \Gamma^T \Gamma)v_{17}, \\
 \bar{\Pi}_6 = & -(D_1v_1)^T F_1 D_1 v_1 - (D_1v_1)^T F_1 D_2 v_4 \\
 & -(D_1v_1)^T F_1 E_2 v_{18} - (D_2v_4)^T F_1 D_1 v_1 \\
 & -(D_2v_4)^T F_1 D_2 v_4 - (D_2v_4)^T F_1 E_2 v_{18} \\
 & -(E_2v_{18})^T F_1 D_1 v_1 - (E_2v_{18})^T F_1 D_2 v_4 \\
 & -2(D_1v_1)^T F_2 v_{18} - 2(D_2v_4)^T F_2 v_{18} \\
 & -v_{18}^T (E_2^T F_1 E_2 + 2E_2^T F_2 + F_3)v_{18}, \\
 \bar{S}_0 = & [\sigma_1(G^{(1)} \otimes B_1) - (I_N \otimes C)]v_1 \\
 & + \sigma_2(G^{(2)} \otimes B_2)v_4 + \sigma_3(G^{(3)} \otimes B_3)v_{17} \\
 & -v_5 + E_1 v_{18},
 \end{aligned}$$

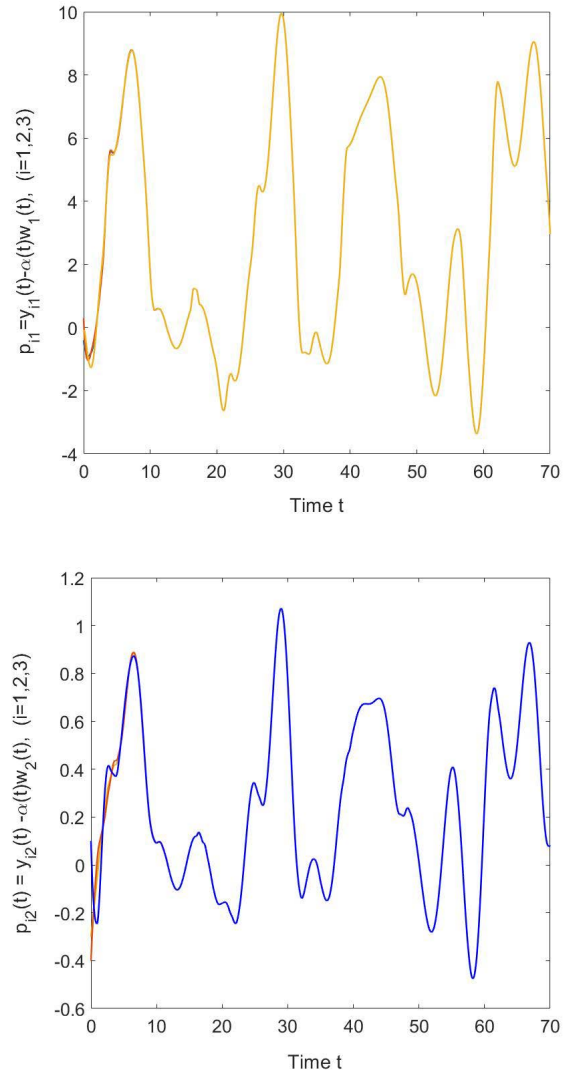


FIGURE 4. The state trajectories of the error system without control in Example 1, where  $p_i(t) = y_i(t) - \alpha(t)w(t)$ , ( $i = 1, 2, 3$ ).

then, the system (12) is asymptotically stable and extended dissipative with the gained sampled-data feedback controller designed as  $K = Z^{-1}Y$ .

*Proof:* To show that the system (12) is extended dissipative, first, we use the LKFs candidate (18) and the following performance index for the system (12). Using inequality (36) in Theorem 1, equation (14), and LMIs (16) we obtain

$$\begin{aligned}
 \dot{V}(p(t), t) - J(t) & \leq \bar{\mathcal{X}}^T(t) \bar{\Upsilon}(\beta) \bar{\mathcal{X}}(t) \leq 0, \\
 \dot{V}(p(t), t) & \leq -J(t),
 \end{aligned} \tag{39}$$

where  $\bar{\Upsilon}(\beta)$  is defined in (37). Then we integrate both sides of the inequality (39) from 0 to  $t \geq 0$  and letting  $\delta \leq -V(p(0), 0)$ , we get

$$\begin{aligned}
 \int_0^t J(s) ds & \geq V(p(t), t) - V(p(0), 0) \\
 & \geq p^T(t) P p(t) + \delta.
 \end{aligned} \tag{40}$$

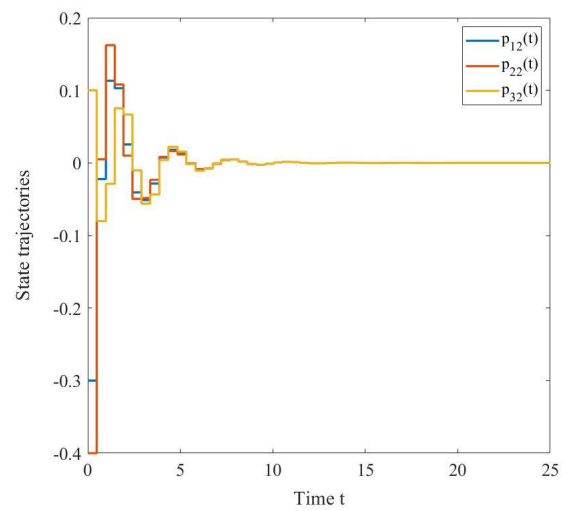
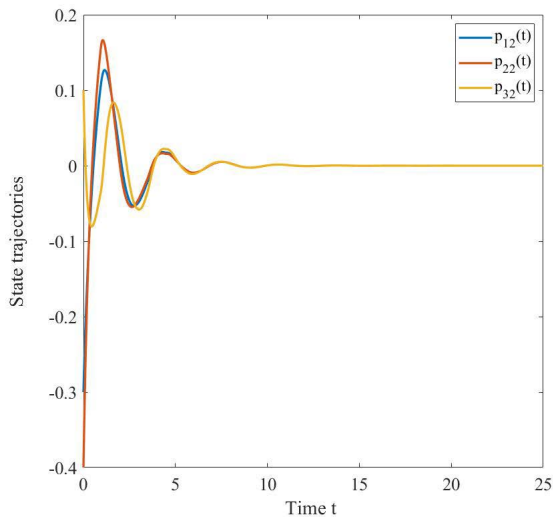
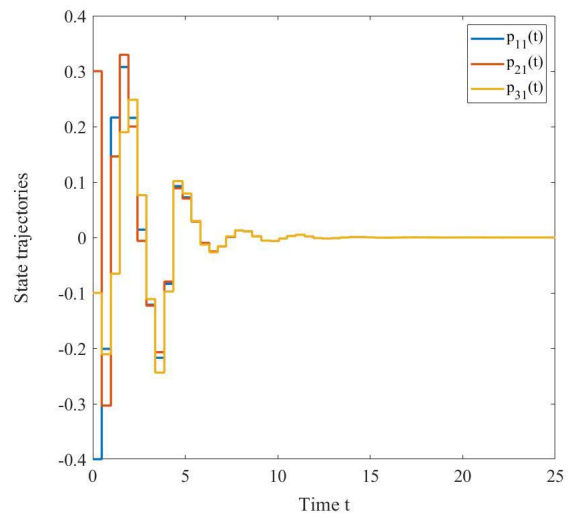
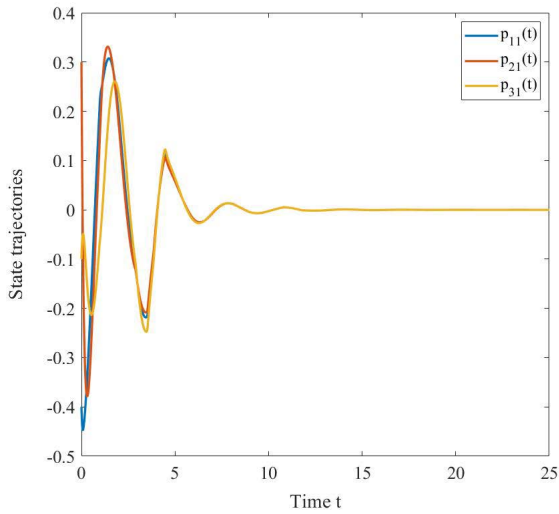


**FIGURE 5.** The state trajectories of the error system with control in Example 1, where  $p_i(t) = y_i(t) - \alpha(t)w(t)$ , ( $i = 1, 2, 3$ ).

**FIGURE 6.** The control input  $u_i(t)$  in Example 1.

Next, we consider two cases:

*Case I:*  $F_4 = 0$ . For this case, from inequality (40) we obtain

$$\int_0^{t_f} J(s) ds \geq \delta. \quad (41)$$

This implies Definition 1 with  $F_4 = 0$ .

*Case II:*  $F_4 \neq 0$ . From Assumption 2, it is clear that  $F_1 = 0, F_2 = 0, F_3 > 0$ , and  $E_2 = 0$ . Then, for any  $0 \leq t \leq t_f$  and  $0 \leq t - \lambda(t) \leq t_f$ , (40) lead to

$$\int_0^{t_f} J(s) ds \geq \int_0^t J(s) ds \geq p^T(t)Pp(t) + \delta, \quad (42)$$

and

$$\begin{aligned} \int_0^{t_f} J(s) ds &\geq \int_0^{t-\lambda(t)} J(s) ds \\ &\geq p^T(t-\lambda(t))Pp(t-\lambda(t)) + \delta. \end{aligned} \quad (43)$$

On the other hand, for  $t - \lambda(t) \leq 0$ , it can be shown that

$$\begin{aligned} &p^T(t-\lambda(t))Pp(t-\lambda(t)) + \delta \\ &\leq \|P\| |p(t-\lambda(t))|^2 + \delta \\ &\leq \|P\| \sup_{-\delta_2 \leq \theta \leq 0} |\phi(\theta)|^2 + \delta \\ &\leq -V(p(0), 0) \\ &\leq \int_0^{t_f} J(s) ds. \end{aligned} \quad (44)$$

Thus, there exists a positive scalar  $\kappa < 1$  such that

$$\begin{aligned} \int_0^{t_f} J(s) ds &\geq \delta + \kappa p^T(t)Pp(t) + (1 - \kappa) \\ &\quad \times p^T(t-\lambda(t))Pp(t-\lambda(t)). \end{aligned} \quad (45)$$

By the relationship of output  $z(t)$  with (38):

$$z^T(t)F_4z(t)$$

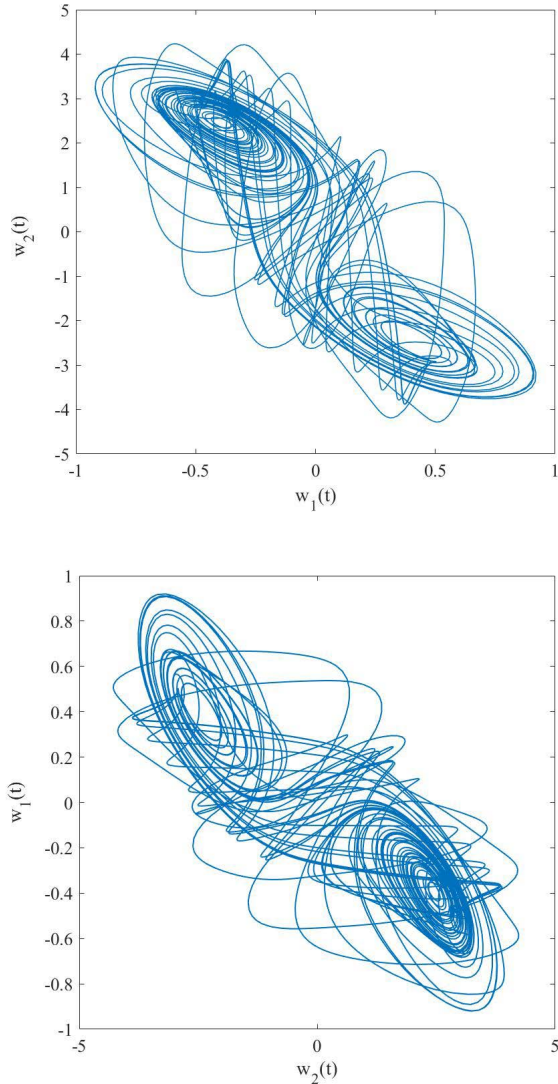


FIGURE 7. The trajectory of the isolated node (48) in Example 2.

$$\begin{aligned}
 &= - \begin{bmatrix} p(t) \\ p(t - \lambda(t)) \end{bmatrix}^T \\
 &\times \begin{bmatrix} \kappa P - D_1^T F_4 D_1 & -D_1^T F_4 D_2 \\ * & (1 - \kappa)P - D_2^T F_4 D_2 \end{bmatrix} \\
 &\times \begin{bmatrix} p(t) \\ p(t - \lambda(t)) \end{bmatrix} + \kappa p^T(t) P p(t) \\
 &+ (1 - \kappa) p^T(t - \lambda(t)) P p(t - \lambda(t)). \tag{46}
 \end{aligned}$$

So, it is clear that for any  $t$  satisfying  $0 \leq t \leq t_f$

$$\int_0^{t_f} J(s) ds \geq z^T(t) F_4 z(t) + \delta. \tag{47}$$

Taking the supremum over  $t$  in inequalities (41) and (47), the system (12) is extended dissipative. This completes the proof.  $\square$

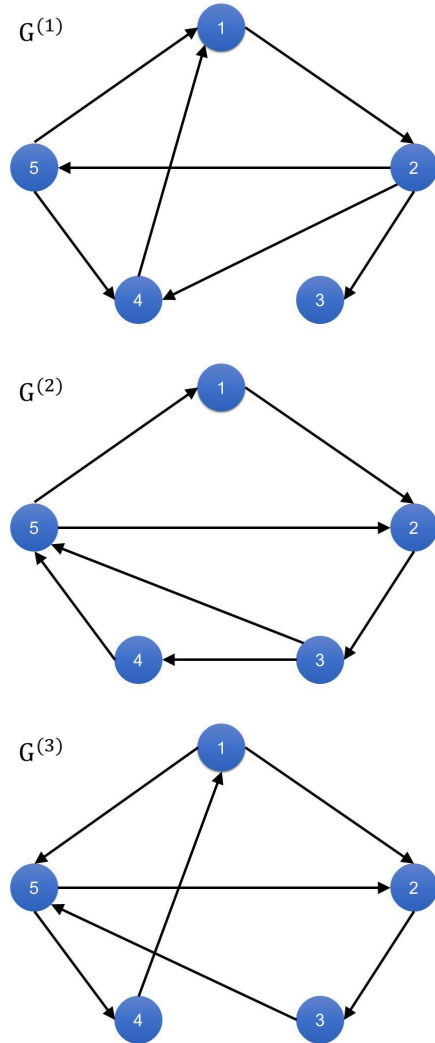


FIGURE 8. Simple directed neural network in Example 2 with 5 nodes.

#### IV. NUMERICAL EXAMPLES

In this section, we provide three examples to illustrate the effectiveness of the results obtained above and applicability of the designed reliable pinning sampled-data controller in the previous section. Now, consider the FPS problem of the following network consisting of two-dimensional NNs (1) and two-dimensional isolated nodes of network by the following equation:

$$\begin{aligned}
 \dot{w}(t) &= -Cw(t) + A_1 f(w(t)) + A_2 f(w(t - r(t))) \\
 &\quad + A_3 \int_{t-d(t)}^t f(w(s)) ds, \tag{48}
 \end{aligned}$$

where  $w(t) = [w_1, w_2]^T \in \mathcal{R}^n$  is the state vector of the network and the parameters  $C, A_1, A_2, A_3, r_1, r_2, d$  and the activation functions will be specified in the following two examples.

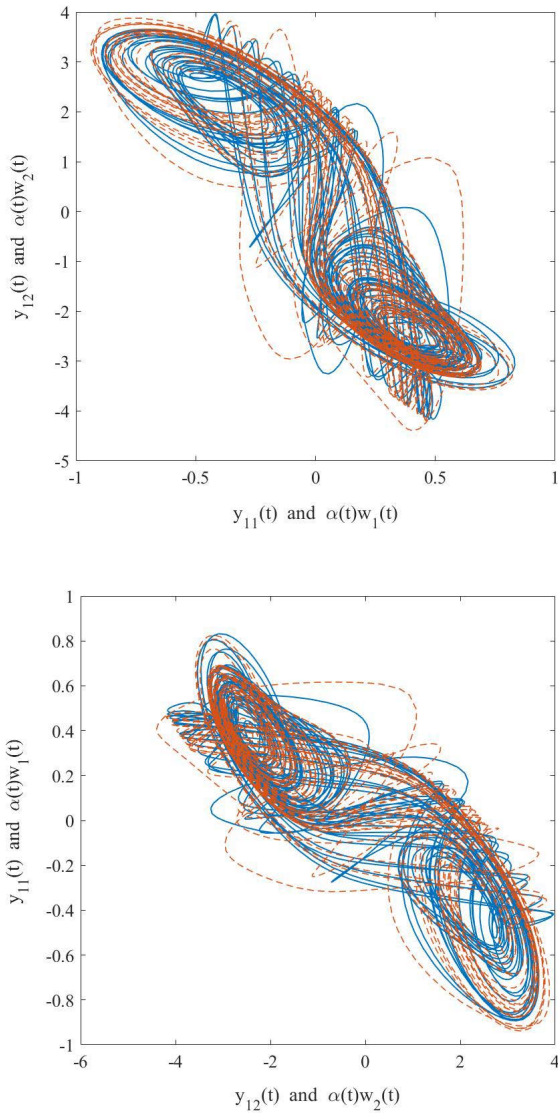


FIGURE 9. The chaotic behavior of the network  $y_i(t)$  and the isolate node  $\alpha(t)w(t)$  in Example 2.

Example 1: Consider the isolated node of network (48) with the parameters as follows:

$$C = \begin{bmatrix} 1 & 0 \\ 0 & 1 \end{bmatrix}, \quad A_1 = \begin{bmatrix} 1.8 & 10 \\ 0.1 & 1.8 \end{bmatrix},$$

$$A_2 = \begin{bmatrix} -1.5 & 0.1 \\ 0.1 & -1.5 \end{bmatrix}, \quad A_3 = \begin{bmatrix} -0.3 & 0.1 \\ 0.1 & -0.2 \end{bmatrix},$$

$f(w_i(t)) = 0.5(|w_i + 1| - |w_i - 1|)$ , ( $i = 1, 2$ ),  $r(t) = 1$ , and  $d(t) = 0.2$ . Then, the trajectory of the isolated node (48) with initial conditions  $w_1(\theta) = 0.9$ ,  $w_2(\theta) = 0.6$ ,  $\forall \theta \in [-1, 0]$  is shown in Figure 1.

As presented in Theorem 1, the pinning sample-data control for FPS of delayed NNs (1) with  $\omega(t) = 0$ , choosing the time-varying scaling function  $\alpha(t) = 0.02 + \cos(\frac{0.1\pi}{1000}t)$ , the coupling strength  $\sigma_1 = 0.2$ ,  $\sigma_2 = 0.1$ ,  $\sigma_3 = 0.5$ , the positive constants  $\epsilon_1 = 0.5$ ,  $\epsilon_2 = 0.5$ ,  $\epsilon_3 = 0.8$ ,  $\epsilon_4 = 0.7$ ,  $\epsilon_5 = 0.8$ ,

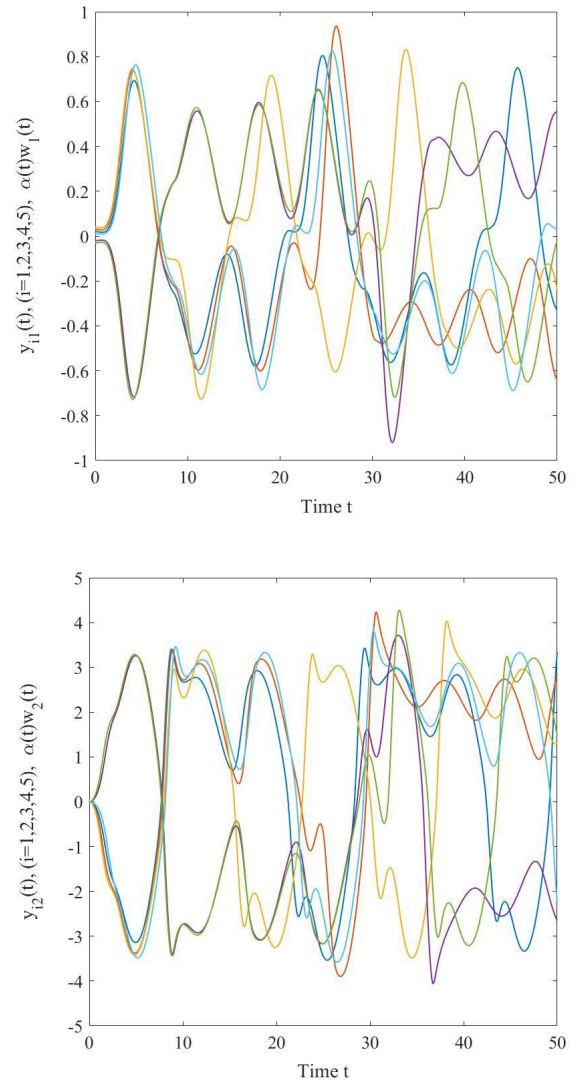


FIGURE 10. The state trajectories of the network  $y_i(t)$ , ( $i = 1, 2, 3, 4, 5$ ) and the isolate node  $\alpha(t)w(t)$  in Example 2.

$\epsilon_6 = 0.6$  the inner-coupling matrices are given by

$$B_1 = \begin{bmatrix} 1 & 0 \\ 0 & 1 \end{bmatrix}, \quad B_2 = \begin{bmatrix} 0.1 & 0 \\ 0 & 0.1 \end{bmatrix},$$

$$B_3 = \begin{bmatrix} 0.2 & 0 \\ 0 & 0.2 \end{bmatrix},$$

and the outer-coupling matrices are described by

$$G^{(1)} = \begin{bmatrix} -2 & 1 & 1 \\ 1 & -2 & 1 \\ 1 & 1 & -2 \end{bmatrix},$$

$$G^{(2)} = \begin{bmatrix} -1 & 0 & 1 \\ 1 & -2 & 1 \\ 1 & 0 & -1 \end{bmatrix},$$

$$G^{(3)} = \begin{bmatrix} -1 & 1 & 0 \\ 0 & -1 & 1 \\ 1 & 1 & -2 \end{bmatrix}.$$

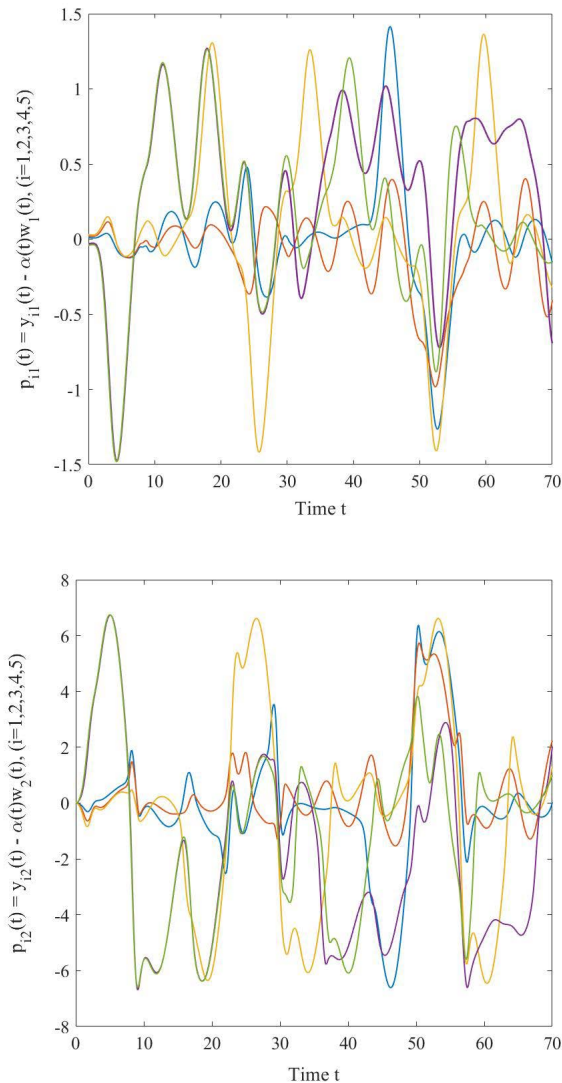


**FIGURE 11.** The state trajectories of the error system without control in Example 2, where  $p_i(t) = y_i(t) - \alpha(t)w_i(t)$ , ( $i = 1, 2, 3, 4, 5$ ).

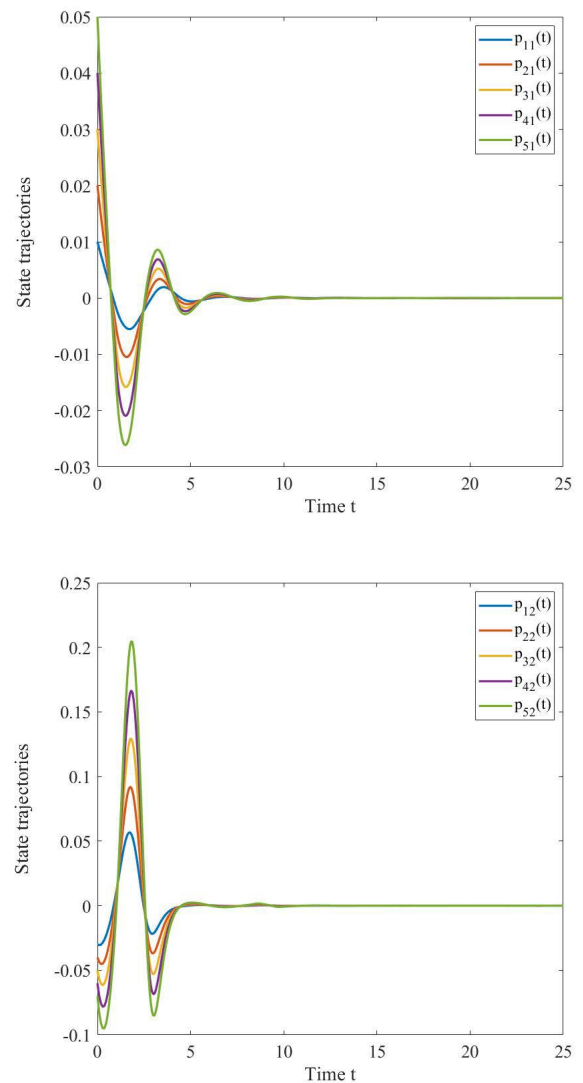


**FIGURE 12.** The state trajectories of the error system with control in Example 2, where  $p_i(t) = y_i(t) - \alpha(t)w_i(t)$ , ( $i = 1, 2, 3, 4, 5$ ).

By solving the LMI (16), the gain matrixes can be obtained as

$$K_1 = \begin{bmatrix} -0.0684 & 0 \\ 0 & -0.0684 \end{bmatrix},$$

$$K_2 = \begin{bmatrix} -0.0452 & 0 \\ 0 & -0.0452 \end{bmatrix},$$

$$K_3 = 0.$$

Moreover, the chaotic behavior of the network  $y_i(t)$  and the isolate node  $w_i(t)$ , ( $i = 1, 2$ ) with the time-varying scaling function  $\alpha(t)$  are shown in Figure 2. Figure 3 shows the state trajectories of the isolated node  $\alpha(t)w_i(t)$  and the network  $y_i(t)$ , ( $i = 1, 2, 3$ ). Figure 4 shows errors between the states of the isolated node  $\alpha(t)w_i(t)$  and the network  $y_i(t)$ , where  $p_{ij}(t) = y_{ij}(t) - \alpha(t)w_j(t)$  ( $i = 1, 2, 3, j = 1, 2$ ) without control (6). In order to illustrate the efficiency of our method, we plot errors between the states of the isolated node  $\alpha(t)w_i(t)$

and network  $y_i(t)$  with control (6) shows in Figure 5, where  $p_{ij}(t) = y_{ij}(t) - \alpha(t)w_j(t)$  ( $i = 1, 2, 3, j = 1, 2$ ). And Figure 6 shows the control input  $u_i(t)$ .

Example 2: In this example, the extended dissipativity performance of the FPS for delayed NNs (1) with pinning sample-data control is considered, which links all of the famous and important performance such as the  $L_2 - L_\infty$ ,  $H_\infty$ , passivity, and dissipativity performances. We consider the isolated node of network (48) with the parameters as follows:

$$C = \begin{bmatrix} 1 & 0 \\ 0 & 1 \end{bmatrix}, \quad A_1 = \begin{bmatrix} 2 & -0.1 \\ -5 & 3 \end{bmatrix},$$

$$A_2 = \begin{bmatrix} -1.5 & 0.1 \\ -0.2 & -2.5 \end{bmatrix}, \quad A_3 = \begin{bmatrix} -0.3 & 0.1 \\ 0.1 & -0.2 \end{bmatrix},$$

$f(w_i(t)) = \tanh(w_i(t))$ , ( $i = 1, 2$ ),  $r(t) = 1$  and  $d(t) = 0.2$ . Then, the trajectory of the isolated node (48) with initial

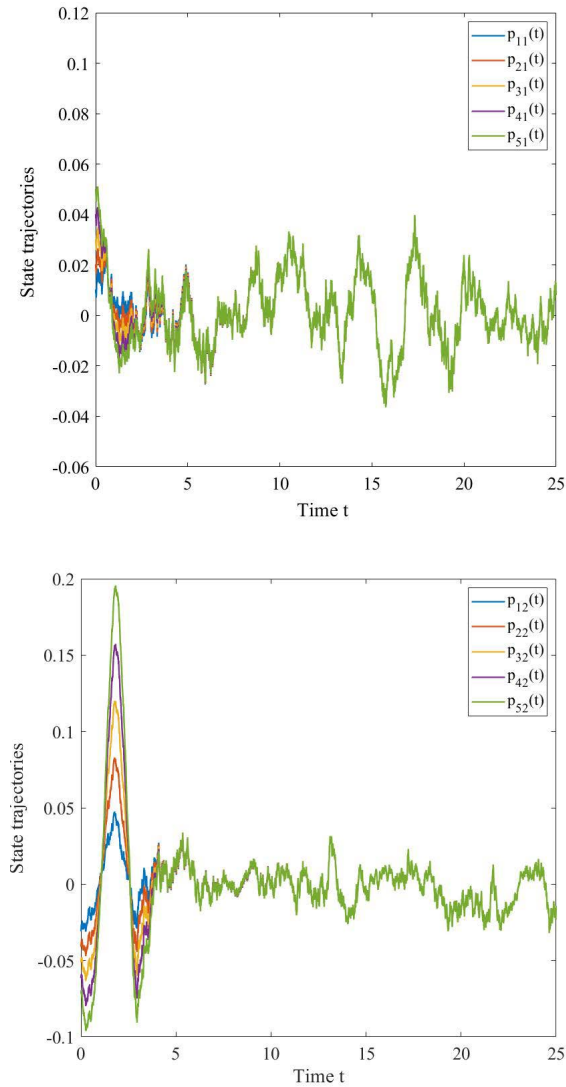


FIGURE 13. The state trajectories of the error system in Example 2 with  $\omega(t)$  is Gaussian noise.

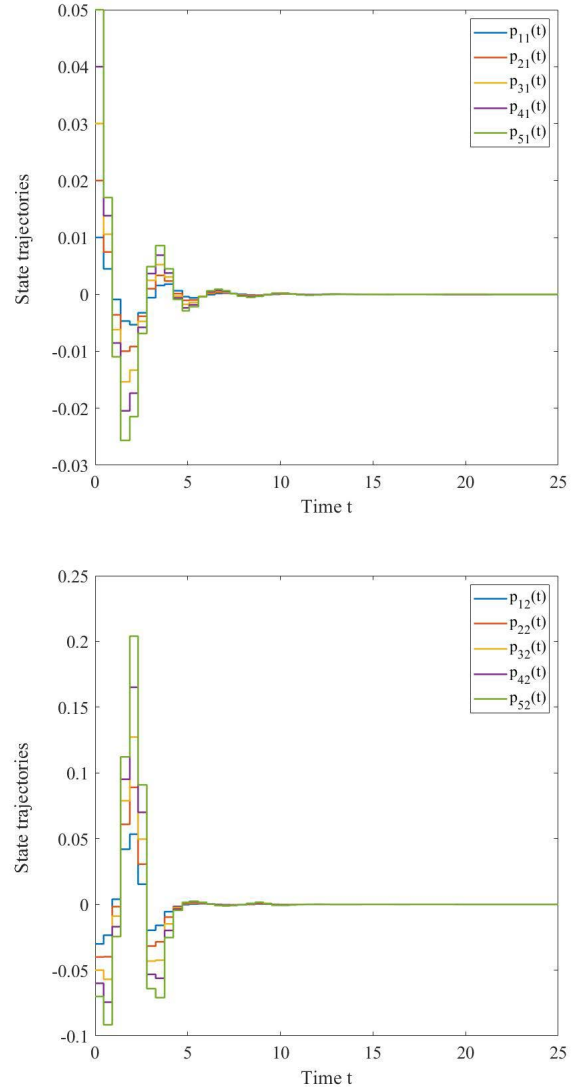


FIGURE 14. The control input  $u_i(t)$  in Example 2.

conditions  $w_1(\theta) = 0.01, w_2(\theta) = 0.01, \forall \theta \in [-1, 0]$  is shown in Figure 7.

As presented in Theorem 2, we consider pinning sample-data control for the FPS of recurrent NNs (1), consisting of fifth linearly coupled identical models (48) with hybrid couplings. Choosing the time-varying scaling function  $\alpha(t) = 0.1 + \cos(\frac{0.5}{100}t)$ , the coupling strength  $\sigma_1 = \sigma_2 = \sigma_3 = 0.1$ , the positive constants  $\epsilon_i = 0.5, (i = 1, 2, \dots, 6), \kappa = 0.5$  and the other parameters are as follows:

$$D_1 = D_2 = E_1 = E_2 = \begin{bmatrix} 1 & 0 \\ 0 & 1 \end{bmatrix},$$

$$\omega(t) = \begin{bmatrix} e^{-0.5t} & 0 \\ 0 & e^{-0.2t} \end{bmatrix}.$$

The inner-coupling matrices are given by

$$B_1 = \begin{bmatrix} 1 & 0 \\ 0 & 1 \end{bmatrix}, B_2 = \begin{bmatrix} 0.1 & 0 \\ 0 & 0.1 \end{bmatrix},$$

$$B_3 = \begin{bmatrix} 0.1 & 0 \\ 0 & 0.1 \end{bmatrix}.$$

The outer-coupling matrices are simple directed NNs as show in Figure 8 and described by

$$G_1 = \begin{bmatrix} -2 & 0 & 0 & 1 & 1 \\ 1 & -1 & 0 & 0 & 0 \\ 0 & 1 & -1 & 0 & 0 \\ 0 & 1 & 0 & -2 & 1 \\ 0 & 1 & 0 & 0 & -1 \end{bmatrix},$$

$$G_2 = \begin{bmatrix} -1 & 0 & 0 & 0 & 1 \\ 1 & -2 & 0 & 0 & 1 \\ 0 & 1 & -1 & 0 & 0 \\ 0 & 0 & 1 & -1 & 0 \\ 0 & 0 & 1 & 1 & -2 \end{bmatrix},$$



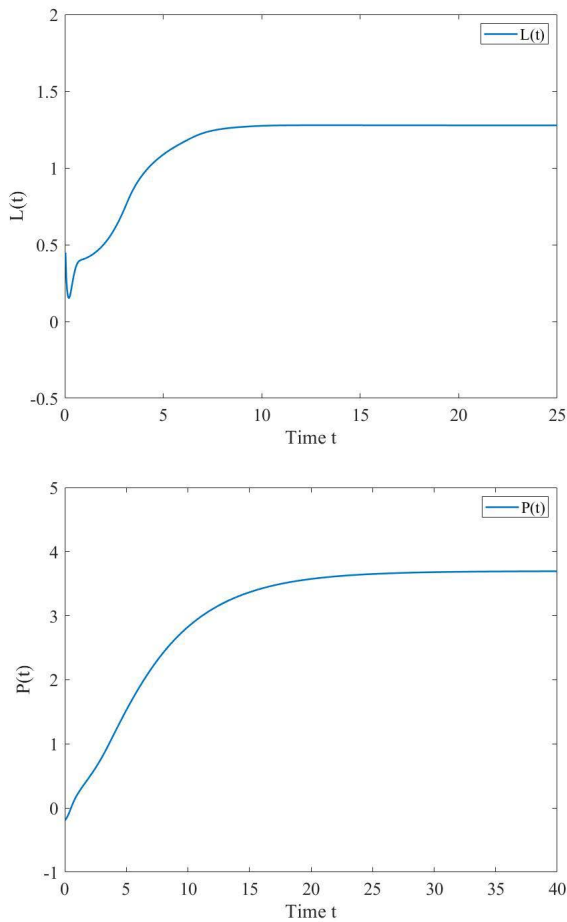


FIGURE 15. The trajectories of  $L(t)$  and  $P(t)$  in Example 2.

$$G_3 = \begin{bmatrix} -1 & 0 & 0 & 1 & 0 \\ 1 & -2 & 0 & 0 & 1 \\ 0 & 1 & -1 & 0 & 0 \\ 0 & 0 & 0 & -1 & 1 \\ 1 & 0 & 1 & 0 & -2 \end{bmatrix}.$$

By solving the LMIs (37)-(38), the gain matrixes can be obtained as

$$K_1 = \begin{bmatrix} -0.0346 & 0 \\ 0 & -0.0346 \end{bmatrix},$$

$$K_2 = \begin{bmatrix} -0.0090 & 0 \\ 0 & -0.0090 \end{bmatrix},$$

$$K_3 = \begin{bmatrix} -0.0366 & 0 \\ 0 & -0.0366 \end{bmatrix},$$

$$K_4 = K_5 = 0.$$

Moreover, the chaotic behavior of the network  $y_i(t)$  and the isolate node  $w_i(t)$ , ( $i = 1, 2$ ) with the time-varying scaling function  $\alpha(t)$  are shown in Figure 9. Figure 10 shows the state trajectories of the isolated node  $\alpha(t)w(t)$  and the network  $y_i(t)$ , ( $i = 1, 2, 3$ ). Figure 11 shows errors between the states of the isolated node  $\alpha(t)w(t)$  and the network  $y_i(t)$ , where  $p_{ij}(t) = y_{ij}(t) - \alpha(t)w_j(t)$  ( $i = 1, 2, 3, j = 1, 2$ ) without control (6). In order to illustrate the efficiency of our method,

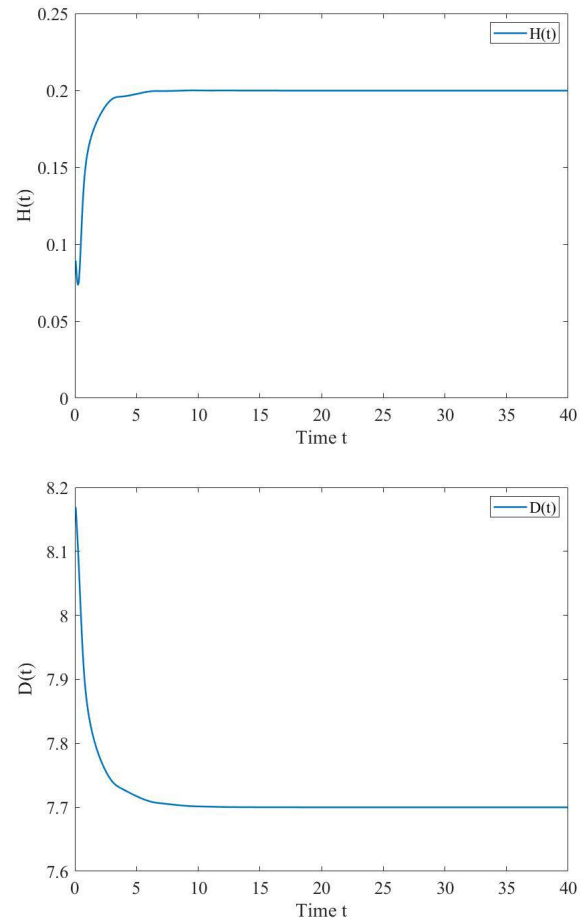


FIGURE 16. The trajectories of  $H(t)$  and  $D(t)$  in Example 2.

we plot errors between the states of the isolated node  $\alpha(t)w(t)$  and network  $y_i(t)$  with control (6) shows in Figure 12, where  $p_{ij}(t) = y_{ij}(t) - \alpha(t)w_j(t)$  ( $i = 1, 2, 3, j = 1, 2$ ). Figure 13 shows the response solution  $p(t)$ , where  $\omega(t)$  is Gaussian noise with mean 0 and variance 1 and the initial condition  $\phi(t) = [-0.2 \ 0.2]^T$ . Figure 14 shows the control input  $u_i(t)$  and for extended dissipative analysis with sample-data control, we consider the following four cases:

Case 1 ( $L_2 - L_\infty$  Performance): By using the LMIs in Theorem 2 and letting  $F_1 = 0, F_2 = 0, F_3 = \gamma^2 I$ , and  $F_4 = I$ , the extended dissipativity performance is converted into the  $L_2 - L_\infty$  performance. Figure 15, shows the plot of  $L(t) = \sqrt{\frac{p^T(t)p(t)}{\int_0^t \omega^T(s)\omega(s)ds}}$ , versus time with the initial condition  $\phi(t) = [0.1 \ 0.1]^T$ . Clearly,  $\sup_{0 \leq t \leq t_f} L(t) = 1.2773$  is less than the prescribed  $L_2 - L_\infty$  performance index 1.5521 in Table 1. The  $L_2 - L_\infty$  performance index  $\gamma$  can be achieved for  $r_1 = 0.5$ , and different  $r_2$ , which are shown in Table 1.

Case 2 (Passivity Performance): By applying the LMIs in Theorem 2 and taking  $F_1 = 0, F_2 = I, F_3 = \gamma I$ , and  $F_4 = 0$ , the extended dissipativity performance degenerates the passivity performance. Figure 15, shows the plot

**TABLE 1. Minimum  $\gamma$  for Case 1. and Case 2. in Example 2 with  $r_1 = 0.5$ , and various  $r_2$ .**

Methods	$r_2 = 0.7$	$r_2 = 0.8$	$r_2 = 0.9$	$r_2 = 1.0$
$L_2 - L_\infty$	1.5521	1.6392	1.7295	1.8171
Passivity	4.3227	4.5231	4.8357	5.1942

**TABLE 2. The maximum allowable values of  $r_2$  for Case 3. and Case 4. in Example 2 with  $r_1 = 0.5$  and various  $\gamma$ .**

Methods	$\gamma = 1.5$	$\gamma = 1.6$	$\gamma = 1.7$	$\gamma = 1.8$
$H_\infty$	0.8511	1.1426	1.3005	1.4893
Dissipativity	1.3178	1.2951	1.2446	1.1996

of  $P(t) = \frac{-2 \int_0^t p^T(s)\omega(s) ds}{\int_0^t \omega^T(s)\omega(s) ds}$ , versus time with the initial condition  $\phi(t) = [0.1 \ 0.1]^T$ . Clearly,  $P(t)$  converges to 3.6932, which is less than the prescribed passivity performance index 4.3227 in Table 1. The passivity performance index  $\gamma$  can be gained for  $r_1 = 0.5$ , and various  $r_2$ , which are presented in Table 1.

Case 3 ( $H_\infty$  Performance): By using the LMIs in Theorem 2 and letting  $F_1 = -I$ ,  $F_2 = 0$ ,  $F_3 = \gamma^2 I$ , and  $F_4 = 0$ , the extended dissipativity performance becomes the  $H_\infty$  performance. Figure 16, shows the plot of  $H(t) = \sqrt{\frac{\int_0^t p^T(s)\omega(s) ds}{\int_0^t \omega^T(s)\omega(s) ds}}$ , versus time with the initial condition  $\phi(t) = [0.1 \ 0.1]^T$ . Clearly,  $H(t)$  converges to 0.1998. The maximum allowable values of  $r_2$  with various  $\gamma$  can be obtained for  $r_1 = 0.5$ , which are depicted in Table 2.

Case 4. Dissipativity performance: By applying the LMIs in Theorem 2 and taking  $F_1 = -I$ ,  $F_2 = I$ ,  $F_3 = \mathcal{R} - \gamma I$ ,  $\mathcal{R} = 8I$ , and  $F_4 = 0$ , the extended dissipativity performance determines the dissipativity performance. Figure 16, shows the plot of  $D(t) = \frac{\int_0^t (-p^T(s)p(s) + 2p^T(s)\omega(s) + 8\omega^T(s)\omega(s)) ds}{\int_0^t \omega^T(s)\omega(s) ds}$ , versus time with the initial condition  $\phi(t) = [0.1 \ 0.1]^T$ . Clearly,  $D(t)$  converges to 7.7000. The maximum allowable values of  $r_2$  with various  $\gamma$  can be achieved for  $r_1 = 0.5$ , which are shown in Table 2.

**V. CONCLUSION**

This research carried out dissipative FPS of NNs with mixed time-varying delays and hybrid couplings. First, we gain novel FPS criteria for delayed hybrid coupled using an appropriate Lyapunov–Krasovskii functional (LKF), a refined Wirtinger single and double integral inequality, and new convex combination lemmas. Furthermore, the coupled NNs and isolated systems could be synchronized up to the desired scaling functions by applying the pinning sampled-data control technique. The FPS result is then used to perform an extended dissipativity analysis, including  $H_\infty$ ,  $L_2 - L_\infty$ , passivity and dissipativity performance, by adjusting parameters in the general index. Eventually, numerical examples are provided to demonstrate the effectiveness of the above theoretical results.

**REFERENCES**

[1] A. Cichoki and R. Unbehauen, *Neural Networks for Optimization and Signal Processing*. Chichester, U.K.: Wiley, 1993.  
 [2] L. O. Chua and L. Yang, “Cellular neural networks: Applications,” *IEEE Trans. Circuits Syst.*, vol. 35, no. 10, pp. 1273–1290, Oct. 1988.

[3] G.-W. You, S. Park, and D. Oh, “Diagnosis of electric vehicle batteries using recurrent neural networks,” *IEEE Trans. Ind. Electron.*, vol. 64, no. 6, pp. 4885–4893, Jun. 2017.  
 [4] M. Ibnkahlia, “Applications of neural networks to digital communications—A survey,” *Signal Process.*, vol. 80, no. 7, pp. 1185–1215, Jul. 2000.  
 [5] Z. Zuo, C. Yang, and Y. Wang, “A new method for stability analysis of recurrent neural networks with interval time-varying delay,” *IEEE Trans. Neural Netw.*, vol. 21, no. 2, pp. 339–344, Feb. 2010.  
 [6] J. Chen, J. Sun, G. P. Liu, and D. Rees, “New delay-dependent stability criteria for neural networks with time-varying interval delay,” *Phys. Lett. A*, vol. 374, pp. 4397–4405, Sep. 2010.  
 [7] Q. Fu, J. Cai, S. Zhong, and Y. Yu, “Dissipativity and passivity analysis for memristor-based neural networks with leakage and two additive time-varying delays,” *Neurocomputing*, vol. 275, pp. 747–757, Jan. 2018.  
 [8] Q. Fu, S. Zhong, W. Jiang, and W. Xie, “Projective synchronization of fuzzy memristive neural networks with pinning impulsive control,” *J. Franklin Inst.*, vol. 357, no. 15, pp. 10387–10409, Oct. 2020.  
 [9] Q. Fu, J. Cai, and S. Zhong, “Robust stabilization of memristor-based coupled neural networks with time-varying delays,” *Int. J. Control, Autom. Syst.*, vol. 17, no. 10, pp. 2666–2676, Oct. 2019.  
 [10] J. Cao, G. Chen, and P. Li, “Global synchronization in an array of delayed neural networks with hybrid coupling,” *IEEE Trans. Syst., Man, Cybern. B, Cybern.*, vol. 38, no. 2, pp. 488–498, Apr. 2008.  
 [11] B. Huang, H. Zhang, D. Gong, and J. Wang, “Synchronization analysis for static neural networks with hybrid couplings and time delays,” *Neurocomputing*, vol. 148, pp. 288–293, Jan. 2015.  
 [12] Y. Xiao, W. Xu, X. Li, and S. Tang, “Adaptive complete synchronization of chaotic dynamical network with unknown and mismatched parameters,” *Chaos, Interdiscipl. J. Nonlinear Sci.*, vol. 17, no. 3, pp. 1–9, Sep. 2007.  
 [13] Z. Zheng and G. Hu, “Generalized synchronization versus phase synchronization,” *Phys. Rev. E, Stat. Phys. Plasmas Fluids Relat. Interdiscip. Top.*, vol. 62, no. 6, pp. 1–4, Dec. 2000.  
 [14] M. G. Rosenblum, A. S. Pikovsky, and J. Kurths, “Phase synchronization of chaotic oscillators,” *Phys. Rev. Lett.*, vol. 76, no. 11, pp. 1–4, Mar. 1996.  
 [15] H. U. Voss, “Anticipating chaotic synchronization,” *Phys. Rev. E, Stat. Phys. Plasmas Fluids Relat. Interdiscip. Top.*, vol. 61, no. 5, pp. 1–5, May 2000.  
 [16] R. Mainieri and J. Rehacek, “Projective synchronization in three-dimensional chaotic systems,” *Phys. Rev. Lett.*, vol. 82, no. 15, pp. 1–4, Apr. 1999.  
 [17] Z. Li and D. Xu, “A secure communication scheme using projective chaos synchronization,” *Chaos, Solitons Fractals*, vol. 22, no. 2, pp. 477–481, Oct. 2004.  
 [18] C. Y. Chee and D. Xu, “Secure digital communication using controlled projective synchronisation of chaos,” *Chaos, Solitons Fractals*, vol. 23, no. 3, pp. 1063–1070, Feb. 2005.  
 [19] P. Niamsup, T. Botmart, and W. Weera, “Modified function projective synchronization of complex dynamical networks with mixed time-varying and asymmetric coupling delays via new hybrid pinning adaptive control,” *Adv. Difference Equ.*, vol. 2017, no. 1, pp. 1–31, Apr. 2017.  
 [20] Y. Chen and X. Li, “Function projective synchronization between two identical chaotic systems,” *Int. J. Mod. Phys. C*, vol. 18, no. 5, pp. 883–888, May 2007.  
 [21] H. Wu, R. Li, R. Yao, and X. Zhang, “Weak, modified and function projective synchronization of chaotic memristive neural networks with time delays,” *Neurocomputing*, vol. 149, pp. 667–676, Feb. 2015.  
 [22] R. Zhang, Y. Yang, Z. Xu, and M. Hu, “Function projective synchronization in drive–response dynamical network,” *Phys. Lett. A*, vol. 374, no. 30, pp. 3025–3028, Jul. 2010.  
 [23] A. Abdurahman, H. Jiang, and Z. Teng, “Function projective synchronization of impulsive neural networks with mixed time-varying delays,” *Nonlinear Dyn.*, vol. 78, no. 4, pp. 2627–2638, Dec. 2014.  
 [24] J. Lu, J. Cao, and D. W. C. Ho, “Adaptive stabilization and synchronization for chaotic Lur’e systems with time-varying delay,” *IEEE Trans. Circuits Syst. I, Reg. Papers*, vol. 55, no. 5, pp. 1347–1356, Jun. 2008.  
 [25] Z. Wu, X. J. Xu, G. Chen, and X. Fu, “Adaptive synchronization and pinning control of colored networks,” *Chaos, Interdiscipl. J. Nonlinear Sci.*, vol. 22, no. 4, pp. 1–9, Dec. 2012.  
 [26] T. Botmart and P. Niamsup, “Exponential synchronization of complex dynamical network with mixed time-varying and hybrid coupling delays via intermittent control,” *Adv. Difference Equ.*, vol. 2014, no. 1, pp. 1–33, May 2014.

- [27] J. Wang, M. Chen, H. Shen, J. H. Park, and Z.-G. Wu, "A Markov jump model approach to reliable event-triggered retarded dynamic output feedback  $H_\infty$  control for networked systems," *Nonlinear Anal., Hybrid Syst.*, vol. 26, pp. 137–150, Nov. 2017.
- [28] X. Yang, J. Cao, and J. Qiu, "Pth moment exponential stochastic synchronization of coupled memristor-based neural networks with mixed delays via delayed impulsive control," *Neural Netw.*, vol. 65, pp. 80–91, May 2015.
- [29] X. F. Wang and G. Chen, "Pinning control of scale-free dynamical networks," *Phys. A, Stat. Mech. Appl.*, vol. 310, nos. 3–4, pp. 524–531, Jul. 2002.
- [30] Q. Song, J. Cao, and F. Liu, "Pinning synchronization of linearly coupled delayed neural networks," *Math. Comput. Simul.*, vol. 86, pp. 39–51, Dec. 2012.
- [31] T. Botmart, N. Yotha, P. Niamsup, and W. Weera, "Hybrid adaptive pinning control for function projective synchronization of delayed neural networks with mixed uncertain couplings," *Complexity*, vol. 2017, pp. 1–18, Aug. 2017.
- [32] D. Gong, F. L. Lewis, L. Wang, and K. Xu, "Synchronization for an array of neural networks with hybrid coupling by a novel pinning control strategy," *Neural Netw.*, vol. 77, pp. 41–50, May 2016.
- [33] S. V. Kumar, S. M. Anthoni, and R. Raja, "Dissipative analysis for aircraft flight control systems with randomly occurring uncertainties via non-fragile sampled-data control," *Math. Comput. Simul.*, vol. 155, pp. 217–226, Jan. 2019.
- [34] Z. Xu, P. Shi, H. Su, Z.-G. Wu, and T. Huang, "Global  $H_\infty$  pinning synchronization of complex networks with sampled-data communications," *IEEE Trans. Neural Netw. Learn. Syst.*, vol. 29, no. 5, pp. 1467–1476, May 2018.
- [35] C. Ma, H. Qiao, and E. Kang, "Mixed  $H_\infty$  and passive depth control for autonomous underwater vehicles with fuzzy memorized sampled-data controller," *Int. J. Fuzzy Syst.*, vol. 20, no. 2, pp. 621–629, Feb. 2018.
- [36] J. Wang, L. Su, H. Shen, Z. G. Wu, and J. H. Park, "Mixed  $H_\infty$ /passive sampled-data synchronization control of complex dynamical networks with distributed coupling delay," *J. Franklin Inst.*, vol. 354, no. 3, pp. 1302–1320, Feb. 2017.
- [37] E. Fridman, A. Seuret, and J.-P. Richard, "Robust sampled-data stabilization of linear systems: An input delay approach," *Automatica*, vol. 40, no. 8, pp. 1441–1446, Aug. 2004.
- [38] S. Dharani, R. Rakkiyappan, and J. H. Park, "Pinning sampled-data synchronization of coupled inertial neural networks with reaction-diffusion terms and time-varying delays," *Neurocomputing*, vol. 227, pp. 101–107, Mar. 2017.
- [39] R. Rakkiyappan, V. P. Latha, and K. Sivaranjani, "Exponential  $H_\infty$  synchronization of Lur'e complex dynamical networks using pinning sampled-data control," *Circuits, Syst. Signal Process.*, vol. 36, no. 10, pp. 3958–3982, Oct. 2017.
- [40] H.-A. Tang, S. Duan, X. Hu, and L. Wang, "Passivity and synchronization of coupled reaction–diffusion neural networks with multiple time-varying delays via impulsive control," *Neurocomputing*, vol. 318, pp. 30–42, Nov. 2018.
- [41] M. V. Thuan, H. Trinh, and L. V. Hien, "New inequality-based approach to passivity analysis of neural networks with interval time-varying delay," *Neurocomputing*, vol. 194, pp. 301–307, Jun. 2016.
- [42] N. Yotha, T. Botmart, K. Mukdasai, and W. Weera, "Improved delay-dependent approach to passivity analysis for uncertain neural networks with discrete interval and distributed time-varying delays," *Vietnam J. Math.*, vol. 45, no. 4, pp. 721–736, Dec. 2017.
- [43] B. Lu, H. Jiang, C. Hu, and A. Abdurahman, "Spacial sampled-data control for  $H_\infty$  output synchronization of directed coupled reaction–diffusion neural networks with mixed delays," *Neural Netw.*, vol. 123, pp. 429–440, Mar. 2020.
- [44] H. D. Choi, C. K. Ahn, P. Shi, M. T. Lim, and M. K. Song, " $L_2 - L_\infty$  filtering for Takagi–Sugeno fuzzy neural networks based on Wirtinger-type inequalities," *Neurocomputing*, vol. 153, pp. 117–125, Apr. 2015.
- [45] J. C. Willems, "Dissipative dynamical systems Part I: General theory," *Arch. Rational Mech. Anal.*, vol. 45, no. 5, pp. 321–351, Jan. 1972.
- [46] Z.-G. Wu, P. Shi, H. Su, and J. Chu, "Dissipativity analysis for discrete-time stochastic neural networks with time-varying delays," *IEEE Trans. Neural Netw. Learn. Syst.*, vol. 24, no. 3, pp. 345–355, Mar. 2013.
- [47] D. Jeltsema and J. M. A. Scherpen, "Tuning of passivity-preserving controllers for switched-mode power converters," *IEEE Trans. Autom. Control*, vol. 49, no. 8, pp. 1333–1344, Aug. 2004.
- [48] Y. Niu, X. Wang, and J. Lu, "Dissipative-based adaptive neural control for nonlinear systems," *J. Control Theory Appl.*, vol. 2, no. 2, pp. 126–130, May 2004.
- [49] Z.-G. Wu, J. Lam, H. Su, and J. Chu, "Stability and dissipativity analysis of static neural networks with time delay," *IEEE Trans. Neural Netw. Learn. Syst.*, vol. 23, no. 2, pp. 199–210, Feb. 2012.
- [50] H.-B. Zeng, J. H. Park, C.-F. Zhang, and W. Wang, "Stability and dissipativity analysis of static neural networks with interval time-varying delay," *J. Franklin Inst.*, vol. 352, no. 3, pp. 1284–1295, Mar. 2015.
- [51] H.-B. Zeng, Y. He, P. Shi, M. Wu, and S.-P. Xiao, "Dissipativity analysis of neural networks with time-varying delays," *Neurocomputing*, vol. 168, pp. 741–746, Nov. 2015.
- [52] Z. Feng and J. Lam, "Stability and dissipativity analysis of distributed delay cellular neural networks," *IEEE Trans. Neural Netw.*, vol. 22, no. 6, pp. 976–981, Jun. 2011.
- [53] B. Zhang, W. X. Zheng, and S. Xu, "Filtering of Markovian jump delay systems based on a new performance index," *IEEE Trans. Circuits Syst. I, Reg. Papers*, vol. 60, no. 5, pp. 1250–1263, May 2013.
- [54] T. H. Lee, M.-J. Park, J. H. Park, O.-M. Kwon, and S.-M. Lee, "Extended dissipative analysis for neural networks with time-varying delays," *IEEE Trans. Neural Netw. Learn. Syst.*, vol. 25, no. 10, pp. 1936–1941, Oct. 2014.
- [55] X. Wang, K. She, S. Zhong, and J. Cheng, "On extended dissipativity analysis for neural networks with time-varying delay and general activation functions," *Adv. Difference Equ.*, vol. 2016, no. 1, pp. 1–16, Dec. 2016.
- [56] R. Manivannan, G. Mahendrakumar, R. Samidurai, J. Cao, and A. Alsaedi, "Exponential stability and extended dissipativity criteria for generalized neural networks with interval time-varying delay signals," *J. Franklin Inst.*, vol. 354, no. 11, pp. 4353–4376, Jul. 2017.
- [57] R. Raja, Q. Zhu, R. Samidurai, S. Senthilraj, and W. Hu, "Improved results on delay-dependent  $H_\infty$  control for uncertain systems with time-varying delays," *Circuits Syst. Signal Process.*, vol. 36, no. 5, pp. 1836–1859, May 2017.
- [58] Z. G. Wu, J. H. Park, H. Su, B. Song, and J. Chu, "Mixed  $H_\infty$  and passive filtering for singular systems with time delays," *Signal Process.*, vol. 93, no. 7, pp. 1705–1711, Jul. 2013.
- [59] L. Su and H. Shen, "Mixed  $H_\infty$ /passive synchronization for complex dynamical networks with sampled-data control," *Appl. Math. Comput.*, vol. 259, pp. 931–942, May 2015.
- [60] D. Zeng, R. Zhang, X. Liu, S. Zhong, and K. Shi, "Pinning stochastic sampled-data control for exponential synchronization of directed complex dynamical networks with sampled-data communications," *Appl. Math. Comput.*, vol. 337, pp. 102–118, Nov. 2018.
- [61] R. Rakkiyappan, G. Velmurugan, J. N. George, and R. Selvamani, "Exponential synchronization of Lur'e complex dynamical networks with uncertain inner coupling and pinning impulsive control," *Appl. Math. Comput.*, vol. 307, pp. 217–231, Aug. 2017.
- [62] K. Gu, J. Chen, and V. L. Kharitonov, *Stability of Time-Delay Systems*. Basel, Switzerland: Birkhäuser, 2003.
- [63] J. Tian, Z. Ren, and S. Zhong, "A new integral inequality and application to stability of time-delay systems," *Appl. Math. Lett.*, vol. 101, pp. 1–7, Mar. 2020.
- [64] Z. Ren and J.-K. Tian, "Stability analysis of systems with interval time-varying delays via a new integral inequality," *Complexity*, vol. 2020, pp. 1–7, Feb. 2020.
- [65] Q. Fu, S. Zhong, and K. Shi, "Exponential synchronization of memristive neural networks with inertial and nonlinear coupling terms: Pinning impulsive control approaches," *Appl. Math. Comput.*, vol. 402, Aug. 2021, Art. no. 126169.



**THONGCHAI BOTMART** received the B.S. degree in mathematics from Khon Kaen University, Khon Kaen, Thailand, in 2002, and the M.S. degree in applied mathematics and the Ph.D. degree in mathematics from Chiang Mai University, Chiang Mai, Thailand, in 2005 and 2011, respectively. He is currently an Associate Professor with the Department of Mathematics, Faculty of Science, Khon Kaen University. His research interests include stability theory of time-delay systems, non-autonomous systems, switched systems, artificial neural networks, complex dynamical networks, synchronization, control theory, and chaos theory.



**WAJAREE WEERA** received the B.S. degree in mathematics, the M.S. degree in applied mathematics, and the Ph.D. degree in mathematics from Chiang Mai University, Chiang Mai, Thailand, in 2005, 2007, and 2015, respectively. She is currently an Assistant Professor with the Department of Mathematics, Faculty of Science, Khon Kaen University. Her research interests include stability theory of time-delay systems, stability analysis, neutral systems, switched systems, and artificial neural networks.



**NARONGSAK YOTHA** received the B.S. degree in mathematics from Khon Kaen University, Khon Kaen, Thailand, in 2004, and the M.S. degree in applied mathematics and the Ph.D. degree in mathematics from Chiang Mai University, Chiang Mai, Thailand, in 2006 and 2014, respectively. He is currently an Assistant Professor with the Department of Applied Mathematics and Statistics, Rajamangala University of Technology Isan. His research interests include stability theory of time-delay systems, artificial neural networks, complex dynamical networks, synchronization, and control theory.



**ARTHIT HONGSRI** received the B.S. degree in mathematics and the M.S. degree in applied mathematics from Khon Kaen University, Khon Kaen, Thailand, in 2017 and 2019, respectively, where he is currently pursuing the Ph.D. degree in mathematics with the Department of Mathematics, Faculty of Science. His research interests include stability of time-delay systems and stability of complex dynamical networks. He has been supported by the Science Achievement Scholarship of Thailand (SAST).



**PIYAPONG NIAMSUP** is currently an Associate Professor with the Department of Mathematics, Faculty of Science, Chiang Mai University, Chiang Mai, Thailand. His research interests include stability of time-delay systems, stability of nonautonomous systems, stability of switched systems, complex dynamical networks, synchronization, and control theory.

...